# RANDOM ACCESS OVER WIRELESS LINKS: OPTIMAL RATE AND ACTIVITY PROBABILITY SELECTION

A THESIS SUBMITTED TO

THE GRADUATE SCHOOL OF ENGINEERING AND SCIENCE

OF BILKENT UNIVERSITY

IN PARTIAL FULFILLMENT OF THE REQUIREMENTS FOR

THE DEGREE OF

MASTER OF SCIENCE

IN

ELECTRICAL AND ELECTRONICS ENGINEERING

By

Nurullah Karakoç

July 2017

Random Access over Wireless Links: Optimal Rate and Activity Probability Selection
By Nurullah Karakoç
July 2017

We certify that we have read this thesis and that in our opinion it is fully adequate, in scope and in quality, as a thesis for the degree of Master of Science.

Tolga Mete Duman (Advisor)

Sinan Gezici

Mehmet Köseoğlu

Approved for the Graduate School of Engineering and Science:

Ezhan Karaşan
Director of the Graduate School

# ABSTRACT

## RANDOM ACCESS OVER WIRELESS LINKS: OPTIMAL RATE AND ACTIVITY PROBABILITY SELECTION

Nurullah Karakoç
M.S. in Electrical and Electronics Engineering
Advisor: Tolga Mete Duman
July 2017

Due to the rapidly increasing number of devices in wireless networks with the proliferation of applications based on new technologies such as machine to machine communications and Internet of Things, there is a growing interest in the random access schemes as they provide a simple means of channel access. To this end, various schemes have been proposed based on the ALOHA protocol to increase the efficiency of the medium access control layer over the last decade. On the other hand, physical layer aspects of random access networks have received relatively limited attention, and there is a need to consider optimal use of the underlying physical layer properties especially for transmission over wireless channels.

In this thesis, we study uncoordinated random access schemes over wireless fading channels where each user independently decides whether to send a packet or not to a common receiver at any given time slot. To characterize the system throughput, i.e., the expected sum-rate, an information theoretic formulation is developed. We consider two scenarios: classical slotted ALOHA, where no multiuser detection (MUD) capability is available and slotted ALOHA with MUD. Our main contribution is that the optimal rates and the channel activity probabilities can be characterized as a function of the user distances to the receiver to maximize the system throughput in each case (more precisely, as a function of the average signal to noise ratios of the users). We use Rayleigh fading as our main channel model, however, we also study the cases where log-normal shadowing is observed along with small scale fading. Our proposed optimal rate selection schemes offer significant increase in expected system throughput compared to the same rate approach commonly used in the literature. In addition to the overall throughput

optimization, the issue of fairness among users is also investigated and solutions which guarantee a minimum amount of individual throughput are developed. We also design systems with limited individual outage probabilities of the users for increased energy efficiency and reduced delay. All of these analytical works are supported with detailed numerical examples, and the performance of the proposed methods are evaluated.

*Keywords:* Random access, Rayleigh fading, shadowing, machine to machine communications, multiple access channel, channel capacity, ALOHA networks, multi user detection, throughput, fairness.

# ÖZET

## KABLOSUZ BAĞLANTILAR ÜZERİNDEN RASTGELE ERİŞİM: EN UYGUN KODLAMA ORANI VE AKTİVİTE OLASILIĞI SEÇİMİ

Nurullah Karakoç
Elektrik Elektronik Mühendisliği, Yüksek Lisans
Tez Danışmanı: Tolga Mete Duman
Temmuz 2017

Makine-makine iletişimi ve Nesnelerin İnterneti gibi yeni teknolojilere dayanan uygulamaların çoğalmasıyla birlikte kablosuz ağlarda hızla artan sayıda aygıttan dolayı basit bir kanal erişimi sağlayan rasgele erişim şemalarına artan bir ilgi var. Bu amaçla, son yıllarda orta erişim kontrol katmanının verimliliğini arttırmak için basit ALOHA protokollerine dayalı çeşitli şemalar önerilmiştir. Öte yandan, rasgele erişim ağlarının fiziksel katman özellikleri, nispeten daha az ilgi toplamıştır ve özellikle kablosuz kanallar üzerinden iletişim için altta yatan fiziksel katman özelliklerinin en uygun şekilde kullanımına ihtiyaç vardır.

Bu tezde, kablosuz sönümlemeli kanallar üzerinden koordine edilmemiş rastgele erişim şemalarını inceliyoruz. Bu şemalarda, her kullanıcı, belirli bir zaman aralığında ortak bir alıcıya paketini göndermek isteyip istemediğini bağımsız olarak kararlaştırır. Sistem verimliliğini yani beklenen toplam kodlama oranını karakterize etmek için bir bilgi kuramı formülasyonu geliştirilmiştir. İki senaryoyu inceliyoruz: çok kullanıcılı algılama yeteneği olmayan klasik zaman dilimli ALOHA ve çok kullanıcılı algılama kapasiteli zaman dilimli ALOHA. Ana katkımız, kullanıcıların optimum kodlama oranları ve kanal etkinlik olasılıklarının, her iki senaryo için de sistem verimliliğini en üst düzeye çıkarmak için alıcıya olan kullanıcı mesafelerinin (daha doğrusu, kullanıcıların sinyal/gürültü oranlarının) bir fonksiyonu olarak karakterize edilebilmesidir. Rayleigh sönümlemeyi ana kanal modelimiz olarak kullanıyoruz, ayrıca log-normal gölgelenmenin küçük ölçekli sönümleme ile birlikte mevcut olduğu durumları inceliyoruz. Önerilen en uygun kodlama oranı seçimi şemalarımız, literatürde yaygın olarak kullanılan aynı oran yaklaşımı ile karşılaştırıldığında beklenen sistem verimliliğinde önemli artış sağlamaktadır. Toplam verimlilik optimizasyonuna ek olarak, kullanıcılar arasındaki adil dağılım problemi de araştırılıp asgari miktarda bireysel verimliliği garanti eden çözümler geliştirilmiştir. Ayrıca, enerji verimliliğini artırmak ve gecikmeyi düşürmek için kullanıcıların kişisel kesilme olasılıklarını sınırlayan sistemleri de tasarlıyoruz. Bütün bu analitik çalışmalar detaylı sayısal örneklerle desteklenmekte ve önerilen yöntemlerin performansı değerlendirilmektedir.

*Anahtar sözcükler*: Rasgele erişim, Rayleigh sönümleme, gölgelendirme, makine-makine iletişimi, çoklu erişim kanalı, kanal kapasitesi, ALOHA ağları, çok kullanıcılı algılama, verimlilik, adil dağılım.

# Acknowledgement

First and foremost, I would like to express my sincere thanks to my thesis advisor Prof. Tolga Mete Duman for his invaluable mentorship and guidance throughout my M.S. study. His wide knowledge and generous support have been of great value for me.

I would also like to thank the Assoc. Prof. Sinan Gezici and Assist. Prof. Mehmet Köseoğlu as my examining committee members for their time and useful comments.

I would like to thank my close friends Umut Demirhan, Kaan Gökcesu, Ömer Burak Demirel and Oğuz Kağan Karakoyun.

I would like to express my thanks to the The Scientic and Technological Research Council of Turkey (TUBITAK) for providing financial support during my M.S. study under the grant 113E223 and BIDEB 2210-E.

I would like to thank my colleagues in the research group Mehdi Dabirnia, Sina Rezaei Aghdam, Mücahit Gümüş, Mahdi Shakiba Herfeh, Alireza Nooraiepour, Serdar Hanoğlu, Ersin Yar and Mert Özateş.

I would also like to thank my family for their invaluable support, motivation and understanding.

# Contents

# List of Figures

# Abbreviations

| | |
|---|---|
| AWGN | Additive White Gaussian Noise |
| CRDSA | Contention Resolution Diversity Slotted ALOHA |
| CSI | Channel State Information |
| i.i.d. | independent and identically distributed |
| IoT | Internet of Things |
| IRSA | Irregular Repetition Slotted ALOHA |
| M2M | Machine to Machine |
| MAC | Multiple Access Channel |
| MPR | Multi Packet Reception |
| MUD | Multi User Detection |
| p.d.f. | probability density function |
| PSD | Power Spectral Density |
| RAN | Random Access Networks |
| SIC | Successive Interference Cancellation |
| SNR | Signal to Noise Ratio |
| w.r.t. | with respect to |

# Symbols

| | |
|---|---|
| $\mathbf{P}(\cdot)$ | Probability |
| $f_X(x)$ | Probability density function of random variable $X$ |
| $\frac{\partial f}{\partial x}$ | Partial derivative with respect to $x$ |
| $C(\cdot)$ | Channel capacity |
| $\lvert \cdot \rvert$ | Absolute value |
| $\lVert . \rVert$ | Euclidean norm |
| $X^n$ | A vector of length $n$ |
| $[\cdot]^T$ | Transpose |
| $W(\cdot)$ | Lambert-$W$ function |
| $\text{erf}(\cdot)$ | Error function |
| $\mathbf{E}[\cdot]$ | Expectation |

# Chapter 1

# Introduction

The number of devices in certain types of networks are expected to become very large in near future with the introduction of 5G systems, especially in machine to machine (M2M) communications and Internet of Things (IoT). For such networks, random access schemes present attractive solutions to the shared receiver (channel) problems due to their distributed and simple nature, and hence, there is growing interest in them in recent years.

With the proliferation of applications requiring random access over wireless links, the traditional solutions should be modified by taking into account the wireless channel characteristics including channel variations, thermal noise, multiuser interference along with the availability of channel state information (CSI), and novel approaches should be devised.

ALOHA networking considers a common receiver that serves many transmitters over a shared wireless channel. In pure ALOHA [1], the transmitters send their packeted information in a completely random manner without any coordination. If these packets collide at the shared receiver, they are assumed as lost. If there is no collision, then the received packet is decoded correctly. An upgraded version, slotted ALOHA proposed in [2] considers division of time into slots, and makes sure that each user sends their packets in synchrony with these time slots. Transmission is again uncoordinated among users. This simplicity makes ALOHA networking an easy to implement random access scheme. On the other hand, because of the collisions (e.g., more than one packet being transmitted in a slot) over the common communication medium, throughputs of ALOHA schemes are highly limited.

In this thesis, we consider a slotted ALOHA scheme with probabilistically active users over wireless fading channels. We formulate optimization of transmission rates and user activity probabilities with the objective of maximizing the system throughput while also guaranteeing fairness among different users. To make a realistic analysis with wireless link considerations, our formulation includes path-loss and small scale (Rayleigh) fading effects. In addition, we also study the effects of log-normal shadowing. We approach the problem from an information-theoretic perspective at the physical layer without making any changes at the medium access control layer of the standard slotted ALOHA framework. To preserve the simple nature of ALOHA, no coordination among users is considered, and sophisticated schemes such as rate splitting and superposition coding are avoided even though they can also be taken into account within the proposed framework.

## 1.1 Literature Review

There is an extensive literature which focuses on collision recovery in random access. Metzner investigates network throughput performance by using the capture effect in [3]. Capture effect occurs if one of the colliding signals has a significantly higher power with respect to (w.r.t.) the others at the receiver. In that case, the signal with the highest power is decoded by treating the others as noise. Ref. [4] presents a detailed capture effect analysis with wireless channel considerations for both wide-band and narrow-band systems. In [5], the authors specifically study the effects of fading on the capture effect performance in terms of the maximum sum-rate.

Decoding of the packets experiencing collisions has become possible with the advancement in multi-packet reception (MPR) capabilities. In MPR, in the event of collision, the aim is to decode as many packets as possible with multi-user detection (MUD) methods. Mollanoori et al. [6] investigate the performance of successive interference cancellation (SIC) in random access networks. SIC is a type of MUD which relies on the capture effect. In this scheme, after the decoding of the most powerful signal, the receiver reconstructs a clean version of this signal and subtracts it from the received signal, and after subtraction, it decodes the second most powerful signal since it is now the signal with the highest power. This process continues iteratively until all the packets are decoded. Another perspective is that by using multiple copies of a packet and iterative decoding algorithms in the medium access control layer, colliding packets can be resolved with SIC among different time slots. This approach is introduced in the method called contention resolution diversity slotted ALOHA (CRDSA) [7] in which each transmitter sends two replicas of the same packet. An extension, irregular repetition slotted ALOHA (IRSA), has also been introduced to increase the throughput of the slotted ALOHA schemes in [8]. For the latter scheme, the users can send more than two copies of their packets probabilistically according a distribution which optimizes the overall throughput.

In a recent publication on physical layer aspects of random access, Medard et. al. [9] provide a method to increase the sum-rate of slotted ALOHA over an additive white Gaussian noise (AWGN) channel with the help of superposition coding and rate splitting. Ref. [10] extends this approach to Rayleigh fading channels. For interference-free wireless networks, i.e., single user channels, [11] investigates maximum achievable coding rates with a constant rate transmission approach and superposition coding. The results reveal that the superposition coding outperforms the constant rate approach, however, it also increases complexity of the receiver.

The authors in [12] present throughput maximization with random arrivals in both coordinated and uncoordinated setups with the same rate assignment to all the users. By using the average outage rate as a constraint in the optimization process, they reduce the average delay. In [13], the authors propose adaptation of the encoding rate according to the channel traffic to improve the system throughput by allowing MUD without taking into account the wireless channel characteristics explicitly. Ref. [14] presents a general formulation of [13] for various channel models from an information theoretic perspective. Specifically, it introduces lower and upper bounds of the channel capacity of random access by using a broadcast approach.

ALOHA schemes have also been studied with cognitive radio in which the users have the ability to sense the other users' states, i.e., whether they are active or not. Ref. [15] investigates the overall throughput with imperfect channel state information by introducing cognitive ALOHA, and in [16], the authors study throughput optimization under random access for cognitive radio applications. Ref. [17] determines the maximum asymptotic stable throughput in a model called opportunistic slotted ALOHA. In this model, the users know their CSI at the physical layer and improve the system throughput with multiuser diversity, while [18] provides a MUD scheme which is based on diversity for random access, and compares the performance of several MUD techniques. Another work [19] study the cross-layer energy minimization problem in underwater ALOHA networks considering the unique transmission properties of the underwater medium. Firstly, they obtain energy-optimum rates for medium access control layer. Then, they formulate a cross-layer optimization problem which jointly optimizes physical and medium access control layers, and compare the performance of these two optimization results in which cross-layer optimization significantly increases energy efficiency.

Further analysis of random access with fading is made in [20], [21] and [22]. Ref. [20] investigates the throughput of slotted ALOHA in a Nakagami/Rician and a Rician/Nakagami environment with the consideration of both minimum carrier-to-interference ratio and minimum carrier-to-noise ratio constraints. Ref. [21] analyses the capture probability and throughput of random access schemes in Rician/Rayleigh environments, and Ref. [22] evaluates the channel throughput in a Nakagami fading environment. In addition, [23] investigates the effects of Rayleigh fading along with shadowing on slotted ALOHA where analysis is done under the assumption of fast fading. Furthermore, Ref. [24] studies the effects of fading for pure ALOHA.

There are also some efforts on the study of fairness among users in random access networks. Ref. [25] investigates the throughput regions w.r.t. the strength of MPR with a two-user slotted ALOHA system where the strength is determined by the probability that both packets are resolved in a two-user collision. The authors also analyze the relationship between the overall throughput and fairness where Gini-index is used as the fairness metric. In addition, [26] investigates fairness with capture at the physical layer, and optimal activity probabilities are characterized w.r.t. capture probability without channel fading.

## 1.2 Thesis Contributions

In this thesis, we consider many probabilistically active users with different distances to a common receiver. The users transmit their packets over a shared wireless channel. We model the channel variations as slow (non-ergodic) Rayleigh fading, and assume that the users transmit their information with a constant rate at the physical layer. We also assume that CSI is only known at the receiver.

We formulate the problem of transmission rate and activity probability optimization with the objective of maximizing the system throughput while also guaranteeing fairness among different users. To make a realistic analysis with wireless link considerations, our formulation includes path-loss and small scale (Rayleigh) fading effects. We approach the problem from an information-theoretic perspective at the physical layer without making any changes at the medium access control layer of the standard slotted ALOHA framework. To preserve the simple nature of ALOHA, no coordination among users is considered, and sophisticated schemes such as rate splitting and superposition coding are avoided. In addition, we also investigate the effects of the log-normal shadowing on the optimal rate selection.

In classical slotted ALOHA networks [1, 2], no MUD capability is available and collisions result in a loss of all colliding packets. That is, each successfully received packet is the result of a point-to-point transmission without any interference. In this work, we first consider this classical setup, and present a closed-form solution to the rate selection problem for each user as a function of its distance to the common destination[1]. We also guarantee a minimum amount of throughput by allowing far away users to send their packets more frequently. We then examine scenarios where the common receiver is endowed with MUD capabilities. We model each collision as a Gaussian multiple access channel (MAC) with fading, and provide methods to obtain optimal rates and activity probabilities at the receiver as a function of the distances of the users while considering fairness among the users in the system. Noting that there exist practical coding schemes with a small number of users (e.g., two users) over a MAC [27], we focus on the cases where at most two users' signals are allowed to collide for successful decoding, however, the proposed approach can be extended to a higher number of colliding packets in a similar manner. We also design systems which limit the maximum outage probabilities to obtain efficient energy consumption and reduced delay for both MUD and no MUD cases.

We specify the differences between our specific contributions and closely related existing works as follows. While the authors in [10] use average capacity to find the optimal transmission rates, in our work, we focus on slow (non-ergodic) fading scenarios and use an outage probability formulation. Also, we emphasize that [9] and [10] employ superposition coding, while we adopt a constant rate approach for a given user throughout its transmission. We also consider cases with MUD capabilities different from the approach in [11]. In [12], the authors consider the same rate approach for all the users, and they use the average outage rate as a constraint in the optimization process, however, in our work, the users can have different rates, and we focus on fairness among users with individual throughputs and outage probabilities rather than considering average outage probability only.

[1]More generally, this can be interpreted as a function of the average signal to noise ratio (which in our setup is only a function of the transmitter-receiver separation and the path-loss exponent when there is no shadowing).

In short, we investigate methods of effective use of the physical layer in random access schemes over wireless channels to improve the system throughput while also providing fairness among users. To summarize, our novel contributions are as follows:

- We conduct throughput optimization with different rates assigned to different users.
- We use instantaneous channel capacity formulation to analyze transmissions over slowly fading channels.
- We design systems with fairness among the users. To this end, optimal activity probabilities of the users are specified.
- We investigate the effects of log-normal shadowing on optimal rate selection.
- We design systems with limited maximum outage probabilities for energy efficiency and reduced delay.

## 1.3 Thesis Outline

The thesis is organized in five chapters. In Chapter 2, we review some important preliminaries. These include the concepts of ALOHA networking and slotted ALOHA along with wireless channel considerations used in the rest of the thesis, i.e., path-loss, shadowing, fading, and capacity of Gaussian and fading channels.

In Chapter 3, we investigate the physical layer aspects of slotted ALOHA with Rayleigh fading. Specifically, we provide closed-form solutions to the problems of the optimal rate and activity probability selection for maximum achievable expected throughput under individual throughput fairness and limited outage probability constraints. We also investigate global optimality of these solutions. Furthermore, we analyze the effects of the shadowing along with Rayleigh fading compared to the case of Rayleigh fading only. We present detailed numerical examples for all of these studies to illustrate our results.

Chapter 4 extends the study in Chapter 3 to the scenarios where MUD capability is available at the receiver side. The chapter starts with a review of MUD. Then, we investigate the problems of the optimal rate selection for 2-level MUD and the optimal activity selection for a fair allocation of the individual throughputs. In the solution of these problems, we propose algorithms that use numerical optimization methods, and we verify their global optimality and convergence with an appropriate convexity analysis. We also extend the limited outage probability study and shadowing effects to the MUD case. Detailed numerical examples are also provided.

Finally, Chapter 5 concludes the thesis and presents directions for future research.

# Chapter 2

# Preliminaries

This chapter covers some important background required in the rest of the thesis. The chapter is organized as follows. Firstly, we introduce the concept of ALOHA networking. Secondly, we cover some important features of wireless channels including path-loss, shadowing and multipath fading. Lastly, we discuss the subject of channel capacity with particular focus on fading channels with AWGN.

## 2.1 ALOHA Networking

ALOHA networking (also known as ALOHAnet) is the first example of packet radio transmission in history. It was developed by N. Abramson in 1970 [1], and the physical system became operational in 1971 at the University of Hawaii which connected different campuses of the University of Hawaii with a packet radio communication system.

After the introduction of ALOHA, many improvements and various schemes based on its basic principles have been developed. These improvements are collected under the title of random access networks (RAN), and they represent some of the most studied subjects on multiple access communications in the literature. Most notable variation is the slotted ALOHA which developed in [2]. Some other important protocols are carrier sense multiple access (CSMA) in [28], diversity ALOHA in [29], dynamic frame slotted ALOHA (DFSA) in [30], CRDSA in [7] and IRSA in [8].

This section covers two of the ALOHA protocols in some detail: the first system introduced at University of Hawaii also known as pure ALOHA and its extension the slotted ALOHA.

Pure ALOHA is the simplest and easy to implement packet radio protocol. Multiple transmitters send their packets to a common receiver at any time randomly with no coordination. If two or more packets collide during the transmission, then all the colliding packets are assumed as lost. If there is no collision, then the particular packet is received correctly. Fig. 2.1 shows an example scheme with three users. In this scheme, collisions can occur partially since the transmissions are not synchronized.

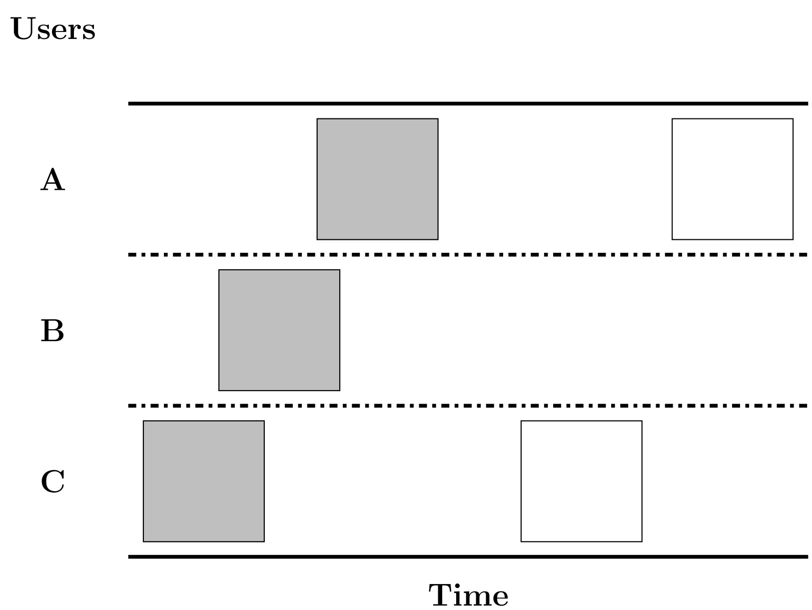


Figure 2.1: Illustration of packet transmission in pure ALOHA. The shaded packets collide while other received correctly in this example.

In order to evaluate the system performance, the common approach is to use success rate of a packet which is called the network throughput and denoted as $T_{pure}$. It is given by $T_{pure} = Ge^{-2G}$ where $G$ is the channel load. The maximum throughput is achieved with $G = 0.5$, resulting in $T^*_{pure} = 1/2e = 0.184$ packets per packet length.

Due to the collisions, the network throughput in pure ALOHA is quite low. In order to increase this, [2] proposes a modification in the system. Namely, it divides the time into slots and makes sure that the packets are transmitted synchronously with these time slots. This scheme is called slotted ALOHA, and it doubles the maximum throughput of pure ALOHA. Fig. 2.2 shows an example with three users. In this scheme, since the transmissions are synchronized, there are no partial collisions among the packets. Collisions occur only if there is more than one packet in a slot. Even though this scheme needs slot synchronization, hence it is more complex, it is still implementable in practice, and it offers a significantly higher performance compared to pure ALOHA.

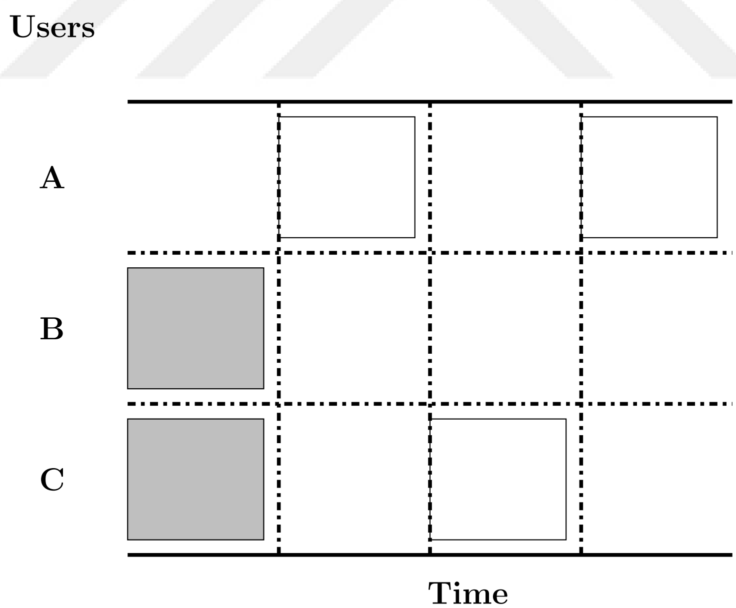


Figure 2.2: Illustration of packet transmission in slotted ALOHA. The shaded packets in the figure collide while the others received correctly.

In order to evaluate the system performance of slotted ALOHA, we use network throughput $T_{SA}$ which is given by $T_{SA} = Ge^{-G}$. The maximum occurs at $G = 1$, and the resulting achievable throughput is $T^*_{SA} = 1/e = 0.368$ packets/slot.

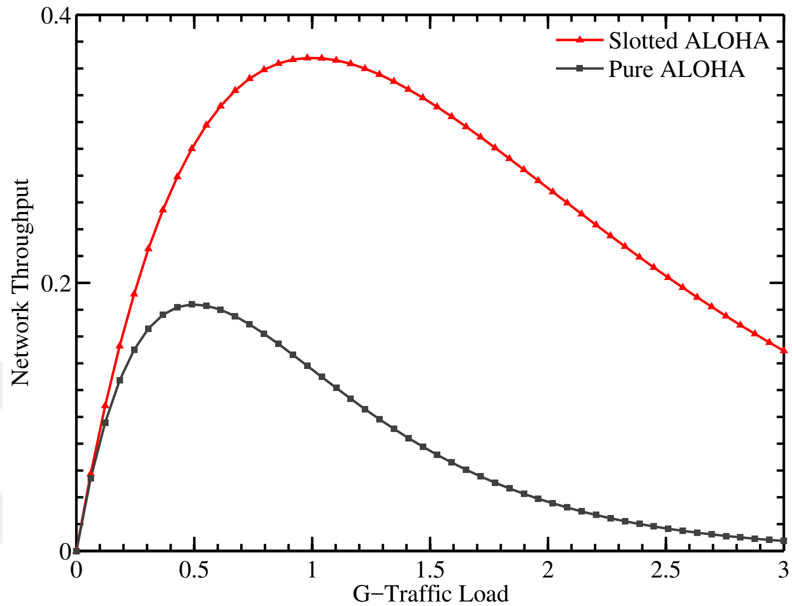


Figure 2.3: Throughputs of pure and slotted ALOHA as a function of the channel load.

Throughput comparison between pure ALOHA and slotted ALOHA is shown in Fig. 2.3. Clearly, the slotted ALOHA has a higher maximum throughput, and offers a much better performance in higher traffic loads compared to pure ALOHA.

## 2.2 Wireless Channels

Wireless channels pose various challenges not observed in wireline communications. These challenges are not only limited to noise and interference, but they also include propagation effects that can change with a random nature. These propagation effects are divided as large-scale and small-scale propagation effects, and they include path-loss, small-scale fading and shadowing [31].

This section covers the effects of path loss, shadowing and fading specifically on the received signal power at the receiver.

### 2.2.1 Large Scale Effects

Throughout the thesis, we use a simplified path-loss model that captures the essence of path-loss propagation without a complicated analysis. In this model, the ratio between the received signal power and the transmitted signal power is given by

$$\frac{P_r}{P_t} = K\left(\frac{d_0}{d}\right)^{\gamma} \tag{2.1}$$

where $K$ is a unitless constant which depends on the antenna characteristics and the average channel attenuation, $d_0$ is a reference distance for the antenna far field, and $\gamma$ is the path loss exponent (for example, $\gamma = 2$ in free space) [31]. These values can be obtained from either an accurate analytical model or an empirical model.

Transmitted signals experience random variations due to blockage from objects, reflecting surfaces and scattering [31]. In order to characterize these variations, we use shadowing as a mathematical model. Most common of which is the log-normal shadowing which is widely used along with the simplified path-loss model. In this case, the ratio of the received to the transmitted power in dB is given by

$$\frac{P_r}{P_t}(dB) = 10\log_{10} K + 10\gamma\log_{10}\left(\frac{d_0}{d}\right) - \psi_{dB} \tag{2.2}$$

where $\psi_{dB}$ is a Gaussian random variable with zero mean and variance $\sigma^2_{\psi_{dB}}$.

Using the standard units, we can also write

$$\frac{P_r}{P_t} = \Psi K\left(\frac{d_0}{d}\right)^{\gamma} \tag{2.3}$$

where $\Psi$ is a log-normal random variable.

### 2.2.2 Small Scale Fading Effects

Along with large scale effects such as path-loss and shadowing, the transmitted signals also experience small scale fading effects in wireless channels. Throughout the thesis, we use Rayleigh model for modeling multi-path fading. Assuming a flat fading channel, using a mathematically equivalent form, we can write

$$r = hx + n \tag{2.4}$$

where $r$ is the received signal, $x$ is the transmitted signal, $h$ is the channel coefficient and $n$ denotes the additive noise. In this model, $h$ is Rayleigh distributed and it captures the effects of multi-path propagation, and its square $h^2$ is exponentially distributed with mean 1 capturing the received signal power distribution. The received signal power $P_i$ is exponentially distributed with probability density function (p.d.f.):

$$f_{P_i}(\phi_i) = \frac{1}{\phi_{si}} exp(-\phi_i/\phi_{si}), \quad \text{for} \quad \phi_i > 0 \tag{2.5}$$

where $\phi_{si}$ is the average received power [10].

## 2.3 Capacity of Gaussian Channels

This section covers the fundamental limits of transmission over Gaussian channels. The term channel capacity defines the maximum rate of communication for which arbitrarily small error probability can be achieved [32]. We consider AWGN channels with slow and fast fading for both single user and multi-user scenarios.

### 2.3.1 AWGN Channel Capacity

The capacity of a real discrete time AWGN channel can be written as

$$C_{AWGN} = \frac{1}{2}\log_2\left(1 + \frac{P}{\sigma^2}\right) \quad \text{bits/channel use} \tag{2.6}$$

where $P$ is the maximum transmit power and $\sigma^2$ is the noise variance.

For a continuous time waveform AWGN channel with bandwidth $W$ Hz, the channel capacity is

$$C_{AWGN} = W\log_2\left(1 + \frac{P}{N_0 W}\right) \quad \text{bits/s} \tag{2.7}$$

where $N_0/2$ is power spectral density (PSD) of the Gaussian noise. We can also write

$$\frac{C_{AWGN}}{W} = \log_2(1 + \text{SNR}) \quad \text{bits/s/Hz} \tag{2.8}$$

which is called the maximum achievable spectral efficiency where $\text{SNR} = \frac{P}{N_0 W}$ denotes signal to noise ratio.

### 2.3.2 Capacity of Fading Channels

#### 2.3.2.1 Slow (Non-Ergodic) Fading Channels

In slow (non-ergodic) fading channels, e.g., when the fading is quasi-static, we cannot use a nonzero rate that can guarantee reliable communication. Considering fading as constant throughout the codewords (quasi-static assumption) the wireless communication systems need a minimum signal to noise ratio $\text{SNR}_{min}$ for proper operation. Below this threshold value, system performance becomes unacceptable [31], and we say that there is an outage. Outage probability $P_{out}$ is defined as the probability that received SNR is below $\text{SNR}_{min}$. Assuming flat fading, conditioned on a realization of channel with coefficient $h$, the instantaneous signal to noise ratio becomes $h^2\mathrm{SNR}$. Assuming that CSI is only available at the receiver side, the maximum instantaneous rate for reliable communication is $\frac{1}{2}\log_2(1+h^2\mathrm{SNR})$ bits/channel use. Hence, we define the outage probability $P_{out}(R)$ for the selected rate $R$ as

$$P_{out}(R) = \mathbf{P}\left(\frac{1}{2}\log_2(1+h^2\mathrm{SNR}) < R\right). \tag{2.9}$$

As an example, for Rayleigh fading channels, we have

$$P_{out}(R) = 1 - e^{(-(2^{2R}-1)/\mathrm{SNR})}. \tag{2.10}$$

#### 2.3.2.2 Ergodic Fading Channels

For ergodic fading channels, the channel experiences different states throughout the transmission of a codeword, and hence there is a positive rate that can guarantee a reliable communication [32]. Assuming that CSI is only available at the receiver side and we have flat fading, the channel capacity for ergodic fading channels is

$$C = \mathbf{E}\left[\frac{1}{2}\log_2(1+h^2\mathrm{SNR})\right] \tag{2.11}$$

where the expectation is over the random channel coefficient $h$.

A comprehensive survey of information theoretical results for transmission over fading channels is presented in [33].

### 2.3.3 Capacity of Gaussian Multiple Access Channels

In MAC, a common receiver serves several transmitters. For a $K$-user MAC, the channel capacity region is defined by $2^K - 1$ inequalities [34]. We can write the capacity of a Gaussian MAC as

$$\sum_{k \in S} R_k < \log_2 \left(1 + \frac{\sum_{k \in S} P_k}{N_0}\right) \quad \text{for all} \quad S \subset \{1, 2, ..., K\} \tag{2.12}$$

where $R_k$ is the rate of the $k$th user, and $P_k$ is its power constraint.

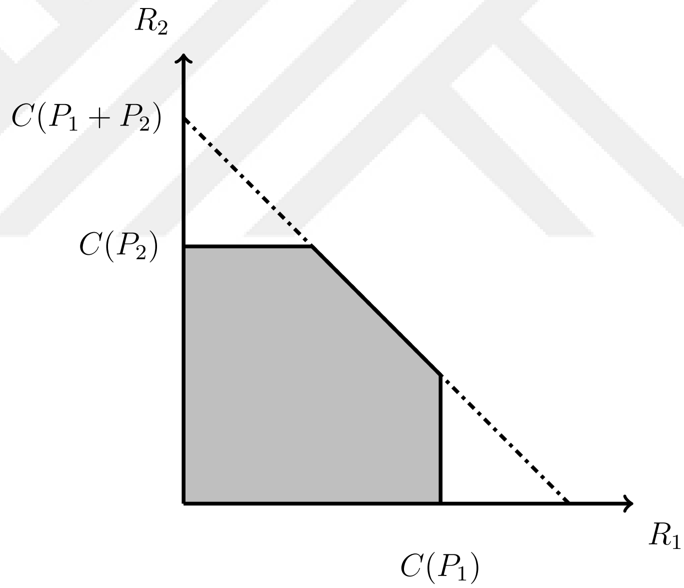


Figure 2.4: Two-user Gaussian MAC capacity region.

For example, in a two-user MAC, the capacity region can be written as

$$\begin{aligned} R_1 &< \frac{1}{2} \log_2 \left(1 + \frac{P_1}{N_0}\right), \\ R_2 &< \frac{1}{2} \log_2 \left(1 + \frac{P_2}{N_0}\right), \\ R_1 + R_2 &< \frac{1}{2} \log_2 \left(1 + \frac{P_1 + P_2}{N_0}\right). \end{aligned} \tag{2.13}$$

Fig. 2.4 illustrates the two-user MAC capacity region. This pentagonal region is determined with the three inequalities in (2.13) along with $R_1, R_2 \geq 0$.

For a Gaussian MAC with two users, conditioned on the real channel gains $h_i$ and $h_j$, and assuming that these channel gains are constant throughout the transmission, the capacity region is

$$\begin{aligned} R_i &< C(P_i h_i^2) \\ R_j &< C(P_j h_j^2) \\ R_i + R_j &< C(P_i h_i^2 + P_j h_j^2) \end{aligned} \tag{2.14}$$

where $(R_i, R_j)$ is the rate pair for the two users, and $C(x) = \frac{1}{2}\log_2(1 + \frac{x}{N})$.

From this characterization one can determine the outage probabilities for given transmission rates. Similarly, one can also write the channel capacity formulation under ergodic fading conditions (omitted).

## 2.4 Chapter Summary

In this chapter, some essential preliminaries such as ALOHA networking along with the wireless channel considerations and the capacity of Gaussian fading channels are reviewed. Firstly, the difference between pure ALOHA and slotted ALOHA, and their performance characteristics are discussed. Then, wireless channel effects such as path-loss, shadowing and fading are covered. Lastly, the important channel capacity formulas with a particular focus on Gaussian and fading channels are stated. In the next chapter, we study the physical layer aspects of slotted ALOHA networks with Rayleigh fading based on these preliminaries.

# Chapter 3

# Slotted ALOHA with Rayleigh Fading

In this chapter, we focus on the physical layer aspects of classical slotted ALOHA networks. Firstly, we investigate the optimal rate selection problem to maximize the system throughput using an information theoretical framework. Our setup includes users with different distances to a common receiver, hence with different average SNRs. We obtain a closed-form solution which reveals an optimal rate selection function w.r.t. the user distances. Secondly, we design a system which ensures individual throughput fairness among the users as a constraint. Our proposed solution adjusts transmission probabilities in order to achieve fairness. Then, we investigate the individual outage probability caused by channel fading, and design a system with limited outage probabilities. Lastly, we consider the effects of shadowing on the rate selection problem.

The chapter is organized as follows: We introduce the system model in the first section. Section 3.2 covers the problem of optimal rate selection. Then, we discuss the issue of fairness in Section 3.3. We study the method of limiting individual probabilities in Section 3.4, and the effects of shadowing in Section 3.5. We present several numerical examples in Section 3.6, and we conclude the chapter with a summary in Section 3.7.

## 3.1 System Model

We consider a slotted ALOHA system over a communication medium characterized as a wireless fading channel with path-loss and small scale fading effects. We assume that there are $n$ users distributed over a ring of inner radius $d_{min}$ and outer radius $d_{max}$, and there is a common receiver at the center of the ring. Fig. 3.1 shows the setup that we use for the user locations. User $i$ is active with probability $p_i$ where $0 \leq p_i \leq 1$, and it has a distance $d_i$ to the common receiver (with $d_{min} \leq d_i \leq d_{max}$).

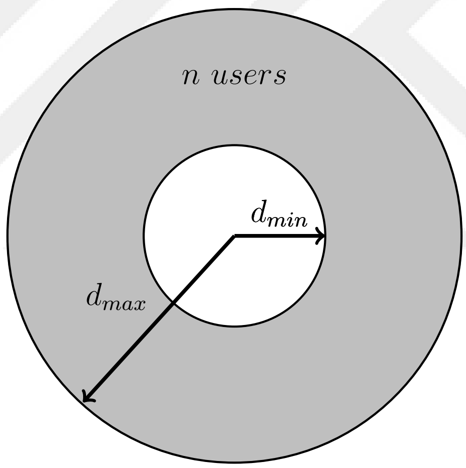


Figure 3.1: Users are distributed on the shaded region.

While we use a simplified path-loss model to determine the average SNR for each user, we note that other channel effects such as shadowing can also be taken into account in the same manner. The received power $P_i$ for the user $i$ is given by

$$P_i = P_t \kappa \left( \frac{d_0}{d_i} \right)^{\gamma} \quad \text{for} \quad i = 1, 2, \ldots, n, \tag{3.1}$$

where $\gamma$ is the path-loss exponent, $P_t$ is the transmission power assumed the same for all the users, $\kappa$ and $d_0$ are constants. To model the small scale fading effects, we consider Rayleigh fading, and assume that the CSI is known at the receiver side only. We also assume that the channel is slowly varying and the channel gain can be modeled as a constant over each time slot (which is long enough to invoke the random coding arguments).

For simplicity of the exposition, we take the channel coefficients as real Rayleigh random variables. Conditioned on the instantaneous (real) channel gain $h_i$, the point-to-point capacity for a (real) AWGN fading channel is

$$C(P_i h_i^2) = \frac{1}{2}\log_2\left(1 + \frac{P_i h_i^2}{N}\right) \quad \text{bits/s/Hz} \tag{3.2}$$

where $C(x) = \frac{1}{2}\log_2(1+\frac{x}{N})$ and $N$ denotes the additive noise power. Hence, with a channel gain of $h_i$, a coding rate $R_i < C(P_i h_i^2)$ can be supported reliably. In addition, we include the effects of shadowing in Section 3.6.

## 3.2 Optimal Rate Selection

In the classical slotted ALOHA without MUD capabilities at the receiver, collisions result in a loss of all the colliding packets. Therefore, achievable rates are identified with the single user capacity in (3.2). We denote $R(d_i)$ as the encoding rate of a user with distance $d_i$ to the common receiver. In order to achieve a successful transmission in a given time slot, there should be only one packet in that particular slot, and the active user's rate should be supported by the specific channel realization. Hence, conditioned on the event that only the user $i$ transmits in a given slot we can write

$$T_i = \begin{cases} R(d_i), & \text{if } R(d_i) < C(P_i h_i^2) \\ 0, & \text{otherwise} \end{cases} \tag{3.3}$$

where $T_i$ shows the throughput of user $i$ in a given slot for the channel gain $h_i$.

### 3.2.1 Problem Definition and Solution

Denoting the expected throughput in a slot by $T$, from the law of total expectation, we obtain

$$\begin{aligned} T &= \sum_{i=1}^{n} (\mathbf{E}_{h_i}[T_i])\mathbf{P}(\text{only } i \text{ transmits}) \\ &= \sum_{i=1}^{n} R(d_i)\mathbf{P}(R(d_i) < C(P_i h_i^2))\mathbf{P}(\text{only } i \text{ transmits}) \end{aligned} \tag{3.4}$$

where $\mathbf{P}(.)$ denotes probability of an event. The expectation $\mathbf{E}_{h_i}[.]$ is taken over the random channel gains resulting in the expected throughput of user $i$ given that only this user transmits in this particular slot. Since transmissions are modeled as independent Bernoulli trials,

$$\mathbf{P}(\text{only } i \text{ transmits}) = p_i \prod_{\substack{j=1 \\ j\neq i}}^{n} (1 - p_j). \tag{3.5}$$

Noting that $h_i^2$ is an exponential random variable, the probability of no outage is given by

$$\begin{aligned} \mathbf{P}(R(d_i) < C(P_i h_i^2)) &= \mathbf{P}_i\left(R(d_i) < \frac{1}{2}\log_2\left(1 + \frac{P_i h_i^2}{N}\right)\right) \\ &= e^{-(2^{2R(d_i)}-1)\frac{N d_i^{\gamma}}{P_0}} \end{aligned} \tag{3.6}$$

with $P_0 = P_t \kappa d_0^{\gamma}$.

By combining (3.4), (3.5) and (3.6), the optimization problem becomes

$$\max_{R(d_i)} \quad \sum_{i=1}^{n} R(d_i) e^{-(2^{2R(d_i)}-1)\frac{N d_i^{\gamma}}{P_0}} p_i \prod_{\substack{j=1 \\ j\neq i}}^{n} (1 - p_j). \tag{3.7}$$

The optimal rate $R^*(d_i)$ of user $i$ can then be characterized as a function of its distance $d_i$ with the help of calculus of variations, specifically, with the

Euler-Lagrange equation which given as

$$\frac{\partial L}{\partial f} - \frac{\partial}{\partial x}\Big(\frac{\partial L}{\partial f'}\Big) = 0 \tag{3.8}$$

where $f = R(d_i)$, $x = d_i$ and $L$ shows the objective function in (3.7). From (3.8), we obtain

$$e^{-(2^{2R^*(d_i)}-1)\alpha_i} p_i \prod_{\substack{j=1 \\ j\neq i}}^{n} (1-p_j)(1-2^{2R^*(d_i)}\alpha_i 2R^*(d_i)\ln 2) = 0 \tag{3.9}$$

with $\alpha_i = \frac{N d_i^\gamma}{P_0}$. Then the optimal rate becomes

$$R^*(d_i) = \frac{W(\frac{P_0}{N d_i^\gamma})}{\ln(4)} \tag{3.10}$$

where $W(.)$ is Lambert-W function[1].

Fig. 3.2 shows an example rate selection curve with respect to the different user distances to the common receiver. In this example, we use 1000 users distributed in the disk with an inner radius of 200 m and outer radius of 1000 m. The average SNR is taken as 8.65 dB and the path-loss exponent is 3.

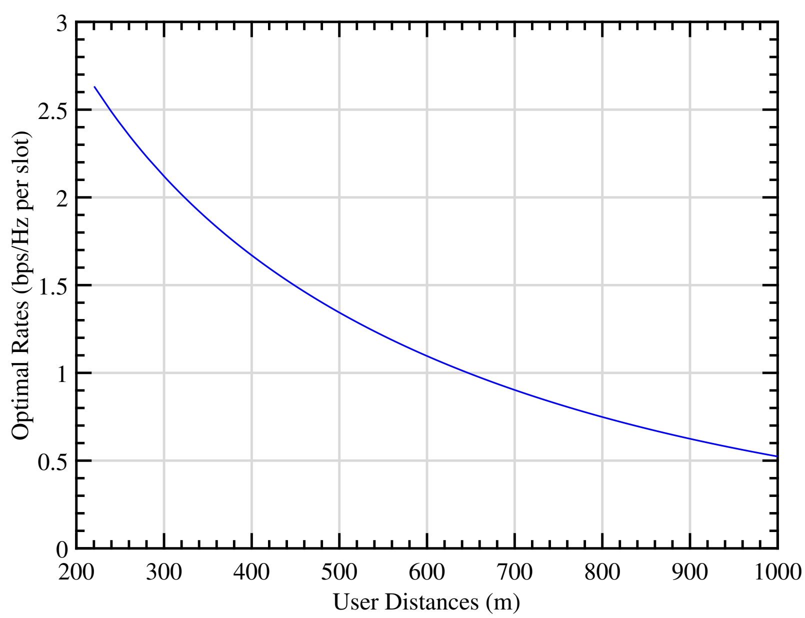


Figure 3.2: Optimal rates vs. user distances for slotted ALOHA over a Rayleigh fading channel.

[1]We note that, this result is derived in [11] as well by using a different approach.

### 3.2.2 Analysis of the Solution

In this section, we verify the global optimality of the solution in (3.10). We denote the system throughput as a summation of the individual throughputs as

$$T = \sum_{i=1}^{n} T_i \tag{3.11}$$

where

$$T_i = R(d_i) e^{-(2^{2R(d_i)}-1)\alpha_i} p_i \prod_{\substack{j=1 \\ j \neq i}}^{n} (1 - p_j).$$

Since $R(d_i)$ values have no effect on $T_j$ when $j \neq i$, we have the optimum system throughput as

$$T^* = \sum_{i=1}^{n} T_i^* \tag{3.12}$$

with

$$T_i^* = \max_{R(d_i)} \quad T_i.$$

The first order partial derivative of $T_i$ w.r.t. $R(d_i)$ can be written as

$$\frac{\partial T_i}{\partial R(d_i)} = e^{-(2^{2R(d_i)}-1)\alpha_i} p_i \prod_{\substack{j=1 \\ j \neq i}}^{n} (1 - p_j)(1 - 2^{2R(d_i)} \alpha_i 2R(d_i) \ln 2). \tag{3.13}$$

Therefore, we obtain

$$\begin{cases} \frac{\partial T_i}{\partial R(d_i)} > 0 & , \quad \text{if } R(d_i) \leq R^*(d_i) = \frac{W(\frac{P_0}{N d_i^{\gamma}})}{\ln(4)}, \\ \frac{\partial T_i}{\partial R(d_i)} \leq 0 & , \quad \text{otherwise.} \end{cases} \tag{3.14}$$

This result indicates that the objective function increases before the optimal point and decreases after, which proves that the result in (3.10) is a globally optimal solution.

## 3.3 System Design with Fairness

The optimal rate function in (3.10) states that the closer users to the destination have higher optimal rates, and hence in the case of identical activity probabilities, i.e., $p_1 = p_2 = \ldots = p_n$, they enjoy higher individual throughputs compared to the far away users. In order to deal with this fairness issue among the users, we propose a method that adjusts the activity probabilities, and we guarantee a minimum amount of individual throughput to each user by allowing far away users to send their packets more frequently.

### 3.3.1 Problem Definition and Solution

For simplicity, the users are divided into $k$ groups in terms of their distances, and we assume that the number of active users in each group in a given slot is modeled as a Poisson random variable with parameter $\lambda_j = n_j p_j$, where $j = 1, 2, \ldots, k$ denotes the group index, and $n_j$ and $p_j$ are number of users and activity probability of each user in the group $j$, respectively. $\lambda_j$ is defined as the $j^{\text{th}}$ group's load and $\sum_{j=1}^{k} \lambda_j$ is the channel load.

The probability that there is only one active user in group $j$ and there are no other active users in the system is $\lambda_j \exp(-\sum_{i=1}^{k} \lambda_i)$. Then, by using (3.7) and

(3.10), the optimization problem can be written as

$$\begin{aligned}
\max_{\lambda_1,\lambda_2,\ldots,\lambda_k} \quad & (e^{-\sum_{i=1}^{k}\lambda_i})\sum_{j=1}^{k}\lambda_j r_j \\
\text{s.t.} \quad & (e^{-\sum_{i=1}^{k}\lambda_i})\lambda_1 r_1 \geq K \\
& (e^{-\sum_{i=1}^{k}\lambda_i})\lambda_2 r_2 \geq K \\
& \vdots \\
& (e^{-\sum_{i=1}^{k}\lambda_i})\lambda_k r_k \geq K \\
& \lambda_1, \lambda_2, ..., \lambda_k \geq 0
\end{aligned} \tag{3.15}$$

where $K$ is the minimum throughput required for each group. $r_j$ is the effective rate of a user in group $j$ given by

$$r_j = R^*(d_j)e^{-(2^{2R^*(d_j)}-1)\frac{Nd_j^{\gamma}}{P_0}}. \tag{3.16}$$

Here $d_j$ denotes the distance of group $j$ users to the receiver assuming that the users in this group have distances to the receiver between $d_j - \delta$ and $d_j + \delta$ with $\delta \ll d_j$, i.e., all the users in the group have the same effective rate.

Notice that $r_j$ is independent of the group load $\lambda_j$, and it can be taken as a constant in this optimization problem. Lagrangian $L$ can be written as

$$L = \sum_{j=1}^{k} -(e^{-\sum_{i=1}^{k}\lambda_i})\lambda_j r_j - \mu_j\lambda_j - \nu_j\Bigg(\lambda_j r_j(e^{-\sum_{i=1}^{k}\lambda_i}) - K\Bigg) \tag{3.17}$$

where $\mu_1, \mu_2, \ldots, \mu_k$ and $\nu_1, \nu_2, \ldots, \nu_k$ are the Lagrange multipliers. We have

$$\begin{aligned}
\nu_j\Bigg(\lambda_j r_j(e^{-\sum_{i=1}^{k}\lambda_i}) - K\Bigg) &= 0, \quad j = 1, 2, \ldots, k \\
\frac{\partial L}{\partial \lambda_j} &= 0, \quad j = 1, 2, \ldots, k \\
\mu_j\lambda_j &= 0, \quad j = 1, 2, \ldots, k.
\end{aligned} \tag{3.18}$$

Hence for $r_1 \geq r_2, ..., r_k$, the optimal group loads are found as

$$\lambda_1 = 1 - \sum_{j=2}^{k} \frac{Ke}{r_j} \quad \text{and} \quad \lambda_j = \frac{Ke}{r_j}, \quad j = 2, 3, ..., k, \tag{3.19}$$

and the optimal activity probabilities of the users in group $j$ are calculated as $p_j = \lambda_j / n_j$ for $j = 1, 2, ..., k$.

We observe that independent of the value of $K$, the optimal channel load is the same all the time, i.e., $\lambda_1 + \lambda_2 + ... + \lambda_k = 1$. In other words, all the groups have just enough load for guaranteeing a throughput of $K$, and then the remaining load is assigned to the group with the highest effective rate $r_j$, i.e., the closest one to the receiver (i.e., the one with the highest average SNR).

### 3.3.2 Analysis of the Solution

In this section, we verify the global optimality of the solution in (3.19). We denote the system throughput as $T = (e^{-\sum_{i=1}^{k} \lambda_i}) \sum_{j=1}^{k} \lambda_j r_j$ and define $T' = -\log(T)$. Then, we have

$$T' = \sum_{i=1}^{k} \lambda_i - \log\left(\sum_{j=1}^{k} \lambda_j r_j\right). \tag{3.20}$$

We can rewrite (3.20) using matrix notation as

$$T' = \mathbf{1}^T \lambda - \log(\mathbf{r}^T \lambda) \tag{3.21}$$

where $\mathbf{1}$ is the column vector of all 1's. $\mathbf{r}$ and $\lambda$ are column vectors of $r_i$'s and $\lambda_i$'s, respectively. We can write

$$\frac{\partial T'}{\partial \lambda} = \mathbf{1}^T - \frac{\mathbf{r}^T}{\mathbf{r}^T \lambda} \tag{3.22}$$

and

$$\frac{\partial^2 T'}{\partial \lambda^2} = \frac{\mathbf{r}^T \mathbf{r}}{(\mathbf{r}^T \lambda)^2} \tag{3.23}$$

which is nonnegative. Therefore, $\log(T)$ is concave, and the system throughput $T$ is log-concave.

Since all of our variables are nonnegative, we can rewrite (3.15) as a convex optimization problem as follows

$$\begin{aligned}
\max_{\lambda_1,\lambda_2,\ldots,\lambda_k} \quad & \log\left((e^{-\sum_{i=1}^{k}\lambda_i})\sum_{j=1}^{k}\lambda_j r_j\right) \\
\text{s.t.} \quad & \log\left((e^{-\sum_{i=1}^{k}\lambda_i})\lambda_1 r_1\right) \geq \log(K) \\
& \log\left((e^{-\sum_{i=1}^{k}\lambda_i})\lambda_2 r_2\right) \geq \log(K) \\
& \vdots \\
& \log\left((e^{-\sum_{i=1}^{k}\lambda_i})\lambda_k r_k\right) \geq \log(K) \\
& \lambda_1, \lambda_2, ..., \lambda_k \geq 0.
\end{aligned} \tag{3.24}$$

The optimal solution of (3.24) is actually the same result obtained in (3.19) which confirms that the global optimality of previous solution.

### 3.3.3 A Different Formulation

We can also consider fully fair system in which all the groups have equal throughputs. Namely, we can solve

$$\begin{aligned}
\max_{\lambda_1,\lambda_2,...,\lambda_k} \quad & K \\
\text{s.t.} \quad & (e^{-\sum_{i=1}^{k}\lambda_i})\lambda_1 r_1 = K \\
& (e^{-\sum_{i=1}^{k}\lambda_i})\lambda_2 r_2 = K \\
& \vdots \\
& (e^{-\sum_{i=1}^{k}\lambda_i})\lambda_k r_k = K \\
& \lambda_1, \lambda_2, ..., \lambda_k \geq 0.
\end{aligned} \tag{3.25}$$

Following similar steps as in the previous subsection, the optimal threshold $K^*$ can be found as

$$K^* = \frac{1}{e}\left(\sum_{i=1}^{k}\frac{1}{r_i}\right)^{-1}, \tag{3.26}$$

while the optimal load $\lambda_j^*$ for each group is given by

$$\lambda_j = \frac{1}{r_j}\left(\sum_{i=1}^{k}\frac{1}{r_i}\right)^{-1}, \tag{3.27}$$

with $j = 1, 2, ..., k$. These results imply that a fully fair system can be achieved by using the users' effective rate only (i.e., their average SNRs).

## 3.4 Limiting Individual Outage Probabilities

Optimal rates in (3.10) may result large outage probabilities for some of the users. Since each outage of a packet leads to a retransmission, it may not be energy efficient or delay efficient to use the rates in (3.10) for some of the users. To handle this issue, we modify the optimization problem in (3.7) by incorporating the individual outage probability constraints. Therefore, the optimization problem becomes

$$\begin{aligned} \max_{R(d_i)} \quad & \sum_{i=1}^{n} R(d_i) e^{-(2^{2R(d_i)}-1)\alpha_i} p_i \prod_{\substack{j=1 \\ j\neq i}}^{n} (1-p_j) \\ \text{s.t.} \quad & 1 - e^{-(2^{2R(d_i)}-1)\alpha_i} \leq \beta_i, \quad \forall i \in \{1, 2, \ldots, n\} \end{aligned} \tag{3.28}$$

where $\beta_i$ is the threshold for the maximum allowed individual outage probability to user $i$. Since each transmission is point-to-point, i.e., independent of each other, we can rewrite (3.28) as

$$\begin{aligned} \max_{R(d_i)} \quad & R(d_i) e^{-(2^{2R(d_i)}-1)\alpha_i} \phi_i \\ \text{s.t.} \quad & 1 - e^{-(2^{2R(d_i)}-1)\alpha_i} \leq \beta_i \end{aligned} \tag{3.29}$$

with $\phi_i = p_i \prod_{\substack{j=1 \\ j\neq i}}^{n} (1-p_j)$.

To solve (3.29), we form the Lagrangian

$$L = -R(d_i) e^{-(2^{2R(d_i)}-1)\alpha_i} \phi_i + \mu (1 - e^{-(2^{2R(d_i)}-1)\alpha_i} - \beta_i) \tag{3.30}$$

where $\mu$ is a Lagrange multiplier. From the KKT conditions, we obtain

$$\begin{gathered} \frac{\partial L}{\partial R(d_i)} = 0 \\ -\left( e^{-(2^{2R(d_i)}-1)\alpha_i} \phi_i (1 - 2^{2R(d_i)} \alpha_i 2R(d_i) \ln 2) \right) + \mu e^{-(2^{2R(d_i)}-1)\alpha_i} 2^{2R(d_i)} \alpha_i 2 \ln 2 = 0 \\ \phi_i - (\phi_i R(d_i) - \mu) 2^{2R(d_i)} \alpha_i 2 \ln 2 = 0 \end{gathered} \tag{3.31}$$

and

$$\mu(1 - e^{-(2^{2R(d_i)}-1)\alpha_i} - \beta_i) = 0, \quad \mu \geq 0. \tag{3.32}$$

By combining (3.31) and (3.32), we obtain the optimal rate of user $i$ as

$$R^*(d_i) = \min\left(\frac{W(\frac{P_0}{Nd_i^\gamma})}{\ln(4)}, \frac{\ln(1 - \frac{\ln(1-\beta_i)}{\alpha_i})}{\ln(4)}\right). \tag{3.33}$$

We also note that limitation of the outage probabilities and fairness can also be combined in a relatively straightforward manner. To do this, we only need to modify the effective rates in the optimization problem of (3.15) w.r.t. (3.33).

## 3.5 Effects of Shadowing

To have a more realistic mathematical model for studying the problem of optimal rate selection, we also include shadowing effects in this section. We follow the same problem definition as in Section 3.2., and we use slow (Rayleigh) fading along with log-normal shadowing.

With shadowing and Rayleigh fading, the instantaneous SNR can be written as $\frac{P_i \Psi_i h_i^2}{N}$ where $\Psi_i$ is a log-normal random variable with parameters $\mu = 0$ and $\sigma^2$, and $h_i^2$ is exponentially distributed with $\lambda = 1$.

Therefore, we can modify the non-outage probability in (3.6) as

$$\begin{aligned}
\mathbf{P}(R(d_i) < C(P_i\Psi_i h_i^2)) &= \mathbf{P}\left(R(d_i) < \frac{1}{2}\log_2\left(1+\frac{P_i\Psi_i h_i^2}{N}\right)\right) \\
&= \mathbf{P}\left(\Psi_i h_i^2 > \frac{N}{P_i}(2^{2R(d_i)}-1)\right) \\
&= P(\Psi_i > z/h_i^2) \\
&= \int_0^\infty f_A(a)\int_{-z/a}^\infty f_{\Psi_i}(\psi) \quad d\psi \quad da \\
&= \int_0^\infty f_A(a)\left(\frac{1}{2}-\frac{1}{2}\mathrm{erf}\left(\frac{\ln(z/a)}{\sqrt{2}\sigma}\right)\right) \quad da \\
&= \int_0^\infty e^{-a}\left(\frac{1}{2}-\frac{1}{2}\mathrm{erf}\left(\frac{\ln(z/a)}{\sqrt{2}\sigma}\right)\right) \quad da
\end{aligned} \tag{3.34}$$

where we have $z = \frac{N}{P_i}(2^{2R(d_i)}-1)$, $a = h_i^2$, and erf(.) denotes the error function.

After this point, we can use numerical tools to compute the last integral in (3.34) for different user distances to find the optimal rates for the users according to their distances to the common receiver. Detailed examples are presented in Section 3.6.4.

## 3.6 Numerical Examples

### 3.6.1 Optimal Rate Selection

A comparison between the throughput performances of various rate selections is given in Fig. 3.3 where we set $\gamma = 3$, $d_{min} = 200m$, $d_{max} = 1000m$, $n = 40000$ and $p_i = 1/40000$ for all the users. We use the optimal rate $R^*(d_i)$ in (3.10), hence we name this scheme the optimal rate method (ORM). We name the approach that uses the rates $R(d_i) = \frac{1}{2}\log_2\left(1+\frac{P_i}{N}\right)$ where $P_i$ is the average received power of user $i$ as the sub-optimal rate method (S-ORM), and the one using the same rate for all the users (equal to the average channel capacity) as the fixed rate method (FRM). The results in Fig. 3.3 clearly show that the proposed solution (ORM) is highly superior in terms of the expected throughput, especially for high SNRs.

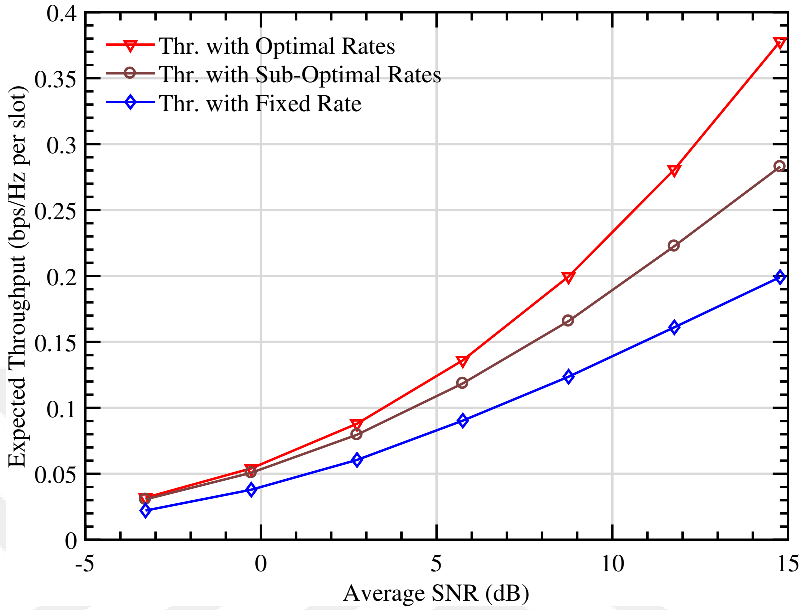


Figure 3.3: Performance comparison for different rate selections (with $\gamma = 3$, $d_{min} = 200$, $d_{max} = 1000$, $n = 40000$ and $p_i = 1/40000$ for all the users).

### 3.6.2 System Design with Fairness

To illustrate how the fairness issue is addressed, we provide an example for $k = 4$ distinct group of users in Fig. 3.4. We set the group load $\lambda_j$ as in (3.19), and the minimum group throughput as $K = 0.06$. Region 1 is the one with the closest users to the common receiver. The plot on the left hand side shows the throughput of the users in each region while the one on the right hand side shows the probability that a user is active in a particular region. Clearly, we can obtain a fair system by only adjusting the activity probabilities. It is also clear that modeling the number of users in each slot as a Poisson random variable is accurate due to the fact that there are a large number of users each with a small activity probability.

Also, to illustrate a fully fair system, an extension of the setup of Fig. 3.4 is studied. According to (3.26), we obtain $K = 0.075$. The corresponding results are provided in Fig. 3.5.

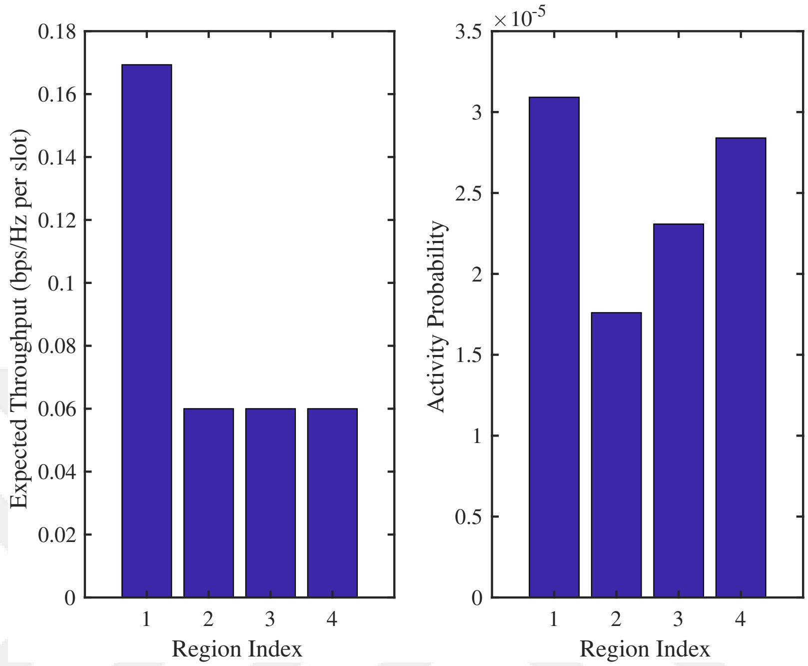


Figure 3.4: A simulation of a fair system with four groups of users (with $\gamma = 3$, $d_{min} = 200m$, $d_{max} = 1000m$, $n = 40000$, average SNR = 8.7 dB).

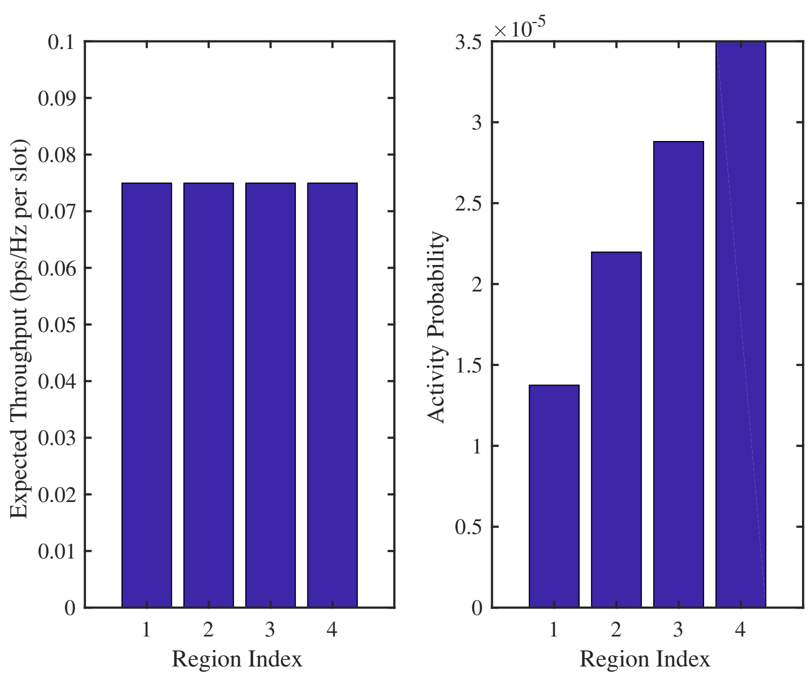


Figure 3.5: A simulation of a fully fair system with four groups of users (with $\gamma = 3$, $d_{min} = 200m$, $d_{max} = 1000m$, $n = 40000$, average SNR = 8.7 dB).

### 3.6.3 Limiting Outage Probabilities

In order to illustrate a design with limited outage probabilities, we use a setup with $n = 100$ users. We use four different outage probability limits ($\beta = 0.1, 0.2, 0.3, 1$) and compare them in terms of the resulting optimal rates in Fig. 3.6. We consider a symmetric setup where $\beta_1 = \beta_2 = \ldots = \beta_n = \beta$. Fig. 3.7 shows the outage probabilities vs. the user distances for the same setup as in Fig. 3.6, while Fig. 3.8 illustrates the individual throughputs corresponding to different maximum outage limits.

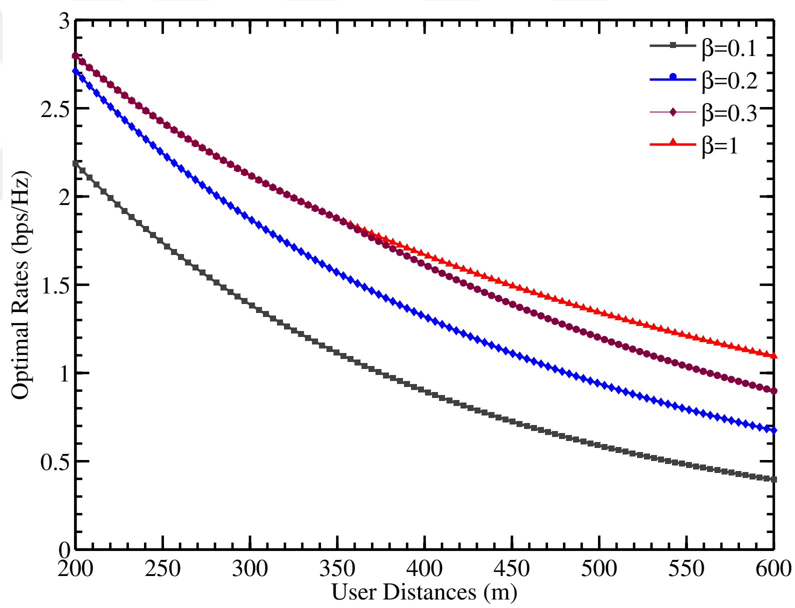


Figure 3.6: Optimal rates with limited maximum outage probabilities (with $\gamma = 3$, $d_{min} = 200m$, $d_{max} = 600m$, average SNR = 8.7 dB).

As shown in Fig. 3.6, to have a more strict outage limitation (i.e., smaller $\beta$), one should decrease the transmission rates which cause lower expected individual throughputs for the users (as shown in Fig. 3.8). However, this policy may be advantageous in terms of energy efficiency and due to delay considerations. In these figures, $\beta = 1$ means that there is no limitation on the outage probabilities, and in this case, the users have different outage probabilities while operating at their optimal rates as illustrated in Fig. 3.7. This figure shows that using a threshold of $\beta = 0.3$ does not cause a change on the optimal rates of the users closer than a distance about 350m and, in this case, the changes on the expected individual throughputs are also relatively small. On the other hand, using a more strict threshold $\beta = 0.1$ causes significant changes on the optimal rates of all the users, and the corresponding expected individual throughputs decrease significantly.

These results reveal that there is a trade-off between the outage probability limits and the expected individual throughputs. This behavior brings out the question of how we should choose the best outage probability threshold $\beta$. The answer is quite dependent on the application. If the application requires high expected throughputs, then the system can be designed with a loose outage probability policy (i.e., with a large $\beta$). On the other hand, if it is a delay or energy consumption sensitive application, the system can be designed with a small $\beta$. We note that the discussions on the energy or delay issues here are limited to the issue of whether a packet is in outage or not. Total energy consumption and total delay calculations are not within the scope of this work.

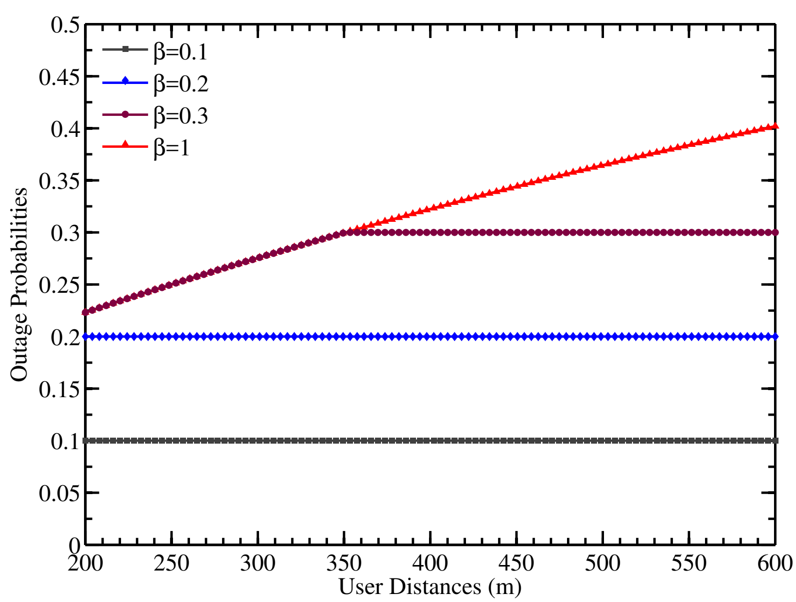


Figure 3.7: Outage probabilities vs. user distances for different outage thresholds (with $\gamma = 3$, $d_{min} = 200m$, $d_{max} = 600m$, average SNR = 8.7 dB).

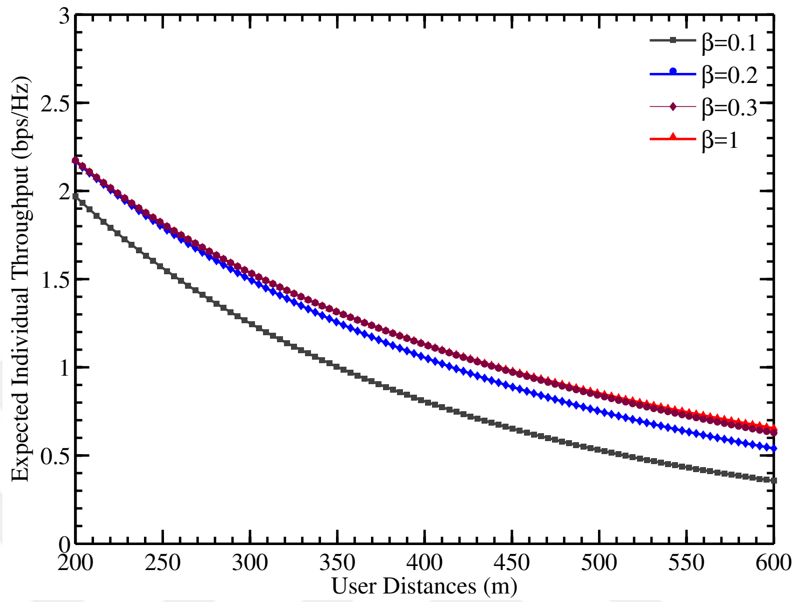


Figure 3.8: Expected individual throughput vs. user distances for different outage thresholds (with $\gamma = 3$, $d_{min} = 200m$, $d_{max} = 600m$, average SNR = 8.7 dB).

### 3.6.4 The Shadowing Effects

To illustrate the effects of shadowing, we use simulations with random variations on the users' SNRs according to log-normal shadowing. Firstly, we present examples for a setup with one user to show the effect of shadowing on a point-to-point communication system. For a user at a distance of 500 m to the receiver, Fig. 3.9 shows the non-outage probability vs. the selected rate for shadowing with $\sigma = 3, 3.65, 4$ dB along with Rayleigh fading. For comparison, the case when there is no shadowing is also presented in the same figure. Fig. 3.10 illustrates the expected throughput vs. the selected rate for the same setup.

These examples represent low SNR scenarios with an average SNR of 2.9 dB. As shown in Fig. 3.9, small changes in the selected rate around the average capacity cause more radical increases or decreases when there is no shadowing compared to the shadowing cases, and when $\sigma$ increases, the non-outage probability becomes less sensitive to the selected rate. The reason behind this is the following: as

$\sigma$ becomes smaller, the variance of the SNR decreases and the instantaneous capacity becomes closer to the average capacity more frequently. For example, if there is neither fading nor shadowing, the behavior turns into a step function in which the non-outage probability turns from 1 to 0 instantly at the rate that equals to the channel capacity since there is no channel randomness.

As shown in Fig. 3.10, shadowing has a supportive role on the expected throughput for a low SNR scenario, and when $\sigma$ increases this role also becomes stronger. The cause of this behavior is that, even at higher rates, the non-outage probability does not decrease as much as the case with no shadowing. This behavior of non-outage event is also the reason of the following observation: as $\sigma$ increases, the optimal rate also increases.

For Fig. 3.11 and Fig. 3.12, we change the user location to 200m and average SNR to 12.3 dB. In Fig. 3.11, we present the non-outage probability vs. the selected rate, and in Fig. 3.12 we illustrate the expected throughput vs. the selected rate. These figures represent a high SNR configuration.

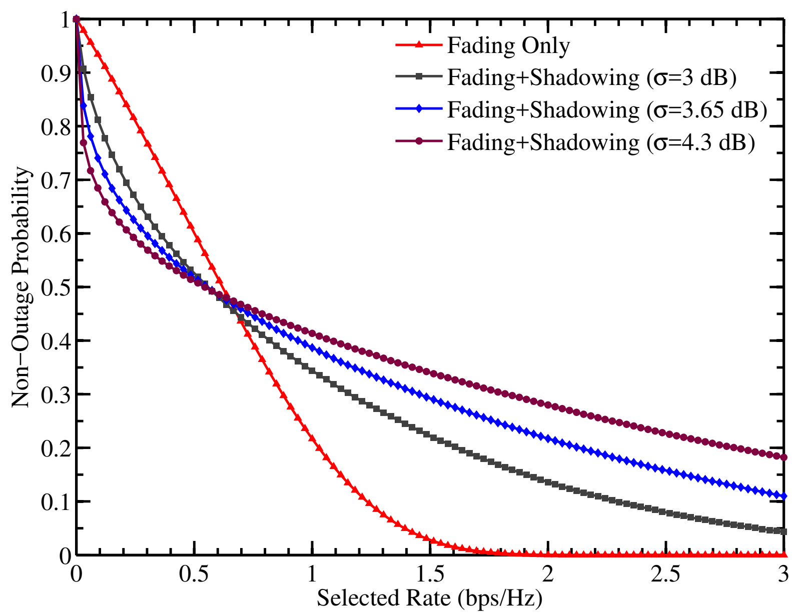


Figure 3.9: Non-outage probability vs. selected rate (with $\gamma = 3.7$, average SNR $= 2.9$ dB).

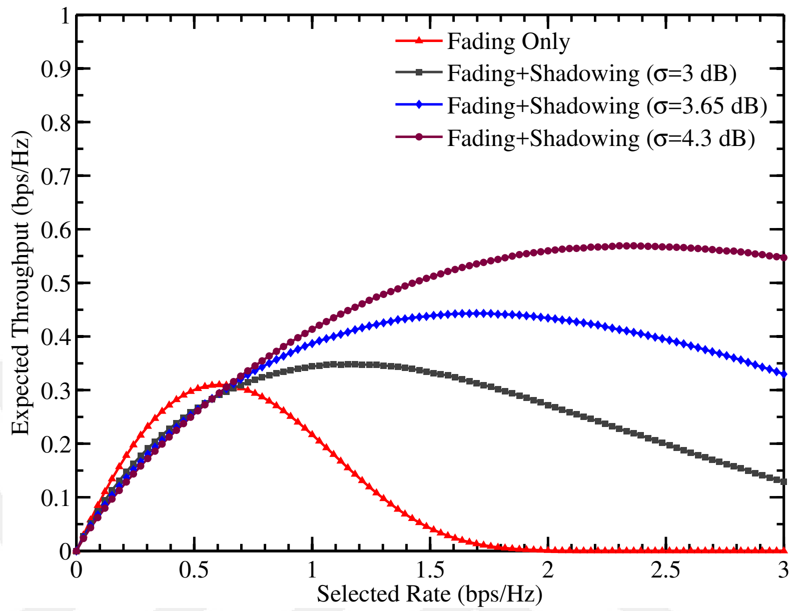


Figure 3.10: Expected throughput vs. selected rate (with $\gamma = 3.7$, average SNR = 2.9 dB).

In the high SNR case, the optimal rates become higher in general, and the decrease in the non-outage probability at low rates become less radical. An important observation is that compared to the low SNR case, shadowing has a destructive role on the expected throughput as in Fig. 3.12. The reason is that $\sigma$ values become smaller compared to the average SNR. The ratio between the variations and average SNR also become smaller and the differences between the optimal rates in the shadowing cases and the optimal rate with no shadowing become relatively small.

To more precisely determine whether shadowing is supportive or destructive, we present Fig. 3.13 and Fig. 3.14. Fig. 3.13 shows the optimal rates which should be selected for the users at different distances. In Fig. 3.14, we present the expected maximum throughputs for different user distances with the optimal rate selection. The results indicate that the critical points between supportive and destructive behavior move towards higher SNRs as $\sigma$ increases.

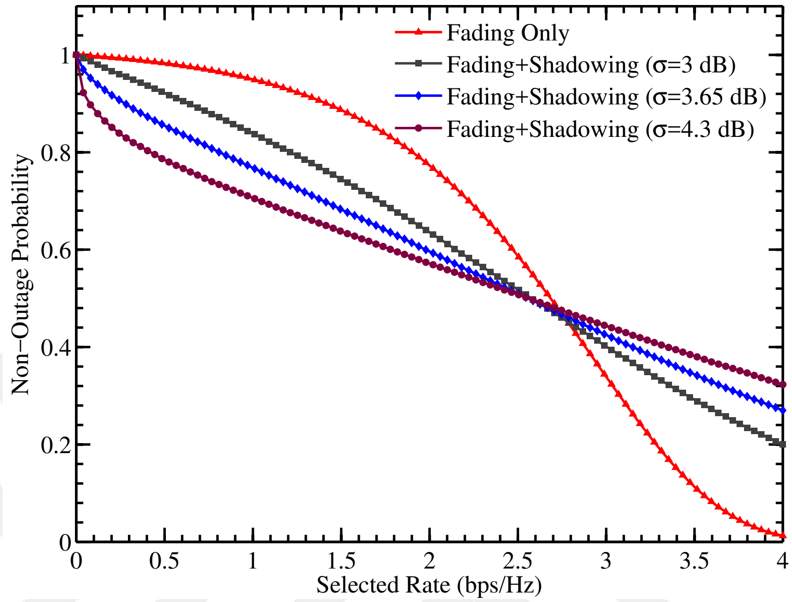


Figure 3.11: Non-outage probability vs. selected rate (with $\gamma = 3.7$, average SNR = 11.1 dB).

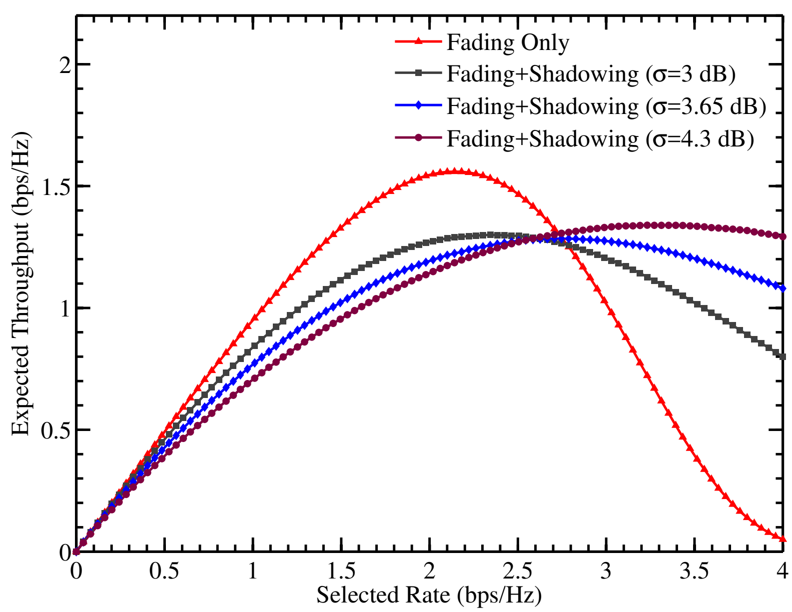


Figure 3.12: Expected throughput vs. selected rate (with $\gamma = 3.7$, average SNR = 11.1 dB).

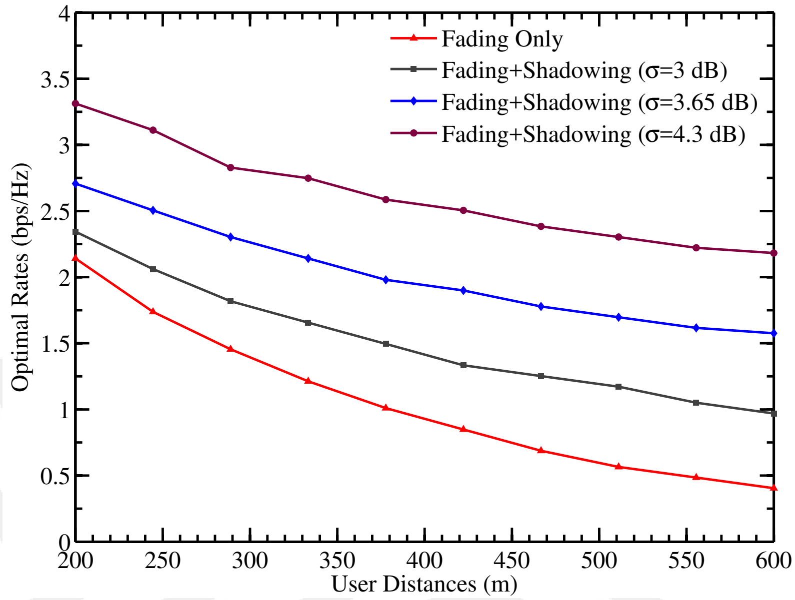


Figure 3.13: Optimal rates vs. user distances (with $\gamma = 3.7$, $d_{min} = 200m$, $d_{max} = 600m$, $\sigma = 3.65$ dB).

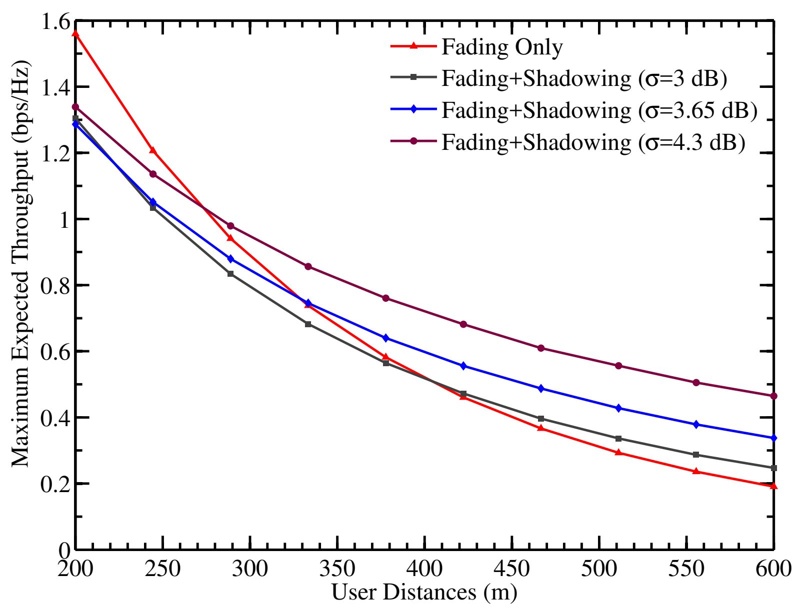


Figure 3.14: Maximum expected throughput vs. user distances (with $\gamma = 3.7$, $d_{min} = 200m$, $d_{max} = 600m$, $\sigma = 3.65$ dB).

## 3.7 Chapter Summary

In this chapter, we have investigated the physical layer aspects of slotted ALOHA networks with Rayleigh fading. We define a model with large number of transmitters with different distances to a common receiver, and we investigate the optimal rates for different users to maximize the overall system throughput. We then examine the individual throughput fairness problem among different users. We also investigate the limited individual outage probabilities of the transmitters, and design a system under fairness and limited outage probability constraints. Lastly, we investigate the effects of shadowing on the optimal rate selection.

Our studies are summarized as follows: We find a closed-form solution to the optimal rate selection problem. The solution indicates an optimal rate selection as a function of the individual distances of the users to the common receiver. We find optimal activity probabilities to guarantee a minimum throughput for each user. We also design a fully fair system where each user has exactly same amount of individual throughput. We verify the global optimality of these solutions. Then, we design a system under limited outage probability constraints. In addition, we also show the effects of the log-normal shadowing on the optimal rate selection. The results indicate that log-normal shadowing is supportive at low SNRs, whereas it is destructive at higher SNRs in terms of the maximum achievable throughputs.

# Chapter 4

# Slotted ALOHA with Multi-User Detection

In this chapter, we extend the findings of the previous chapter to the cases where MUD is available at the receiver side. We start with a brief review of MUD, and we study optimal rate selection problem for this case. Then, we investigate system design under throughput fairness among users and limited outage probability constraints. We also investigate the effects of shadowing. Lastly, we present detailed numerical examples to illustrate our findings.

The chapter is organized as follows: We briefly introduce the concept of MUD in the first section. Section 4.2 covers the problem of optimal rate selection. Then, we discuss the issue of fairness in Section 4.3. We study the method of limiting outage probability in Section 4.4, and the effects of shadowing in Section 4.5. We present several numerical examples in Section 4.6, and we conclude the chapter with a summary in Section 4.7.

## 4.1 Multi-User Detection

MUD deals with demodulation of interfering signals in wireless communications [35]. It aims to decode interfering signals without using methods of resource allocation such as frequency division multiple access (FDMA) and time division multiple access (TDMA).

In this chapter, rather than focusing the methods of the MUD such as successive interference cancellation (SIC), rate splitting and time sharing, we focus on the optimal rate selection and activity probabilities with an information theoretic perspective.

We assume that the fading is slow (non-ergodic), and the CSI is only available at receiver side. Using (2.13), for a Gaussian MAC with two users, conditioned on the real channel gains $h_i$ and $h_j$, and assuming that they are constant over a time slot, the capacity region is

$$\begin{aligned} R_i &< \frac{1}{2}\log_2\left(1+\frac{P_i h_i^2}{N}\right) \\ R_j &< \frac{1}{2}\log_2\left(1+\frac{P_j h_j^2}{N}\right) \\ R_i + R_j &< \frac{1}{2}\log_2\left(1+\frac{P_i h_i^2 + P_j h_j^2}{N}\right) \end{aligned} \tag{4.1}$$

where $(R_i, R_j)$ is the rate pair for the two users.

Fig. 4.1 illustrates two different realizations of the capacity region for two different set of channel realizations. All the rate pairs supporting a reliable communication are in the shaded pentagonal regions represented in (4.1). The selected rate pair $(R_1, R_2)$ that is marked in the figure can be supported for the example on the left hand side, while it is outside the capacity region for the example on the right hand side. Namely, for the latter case the users experience outage due to channel fading.

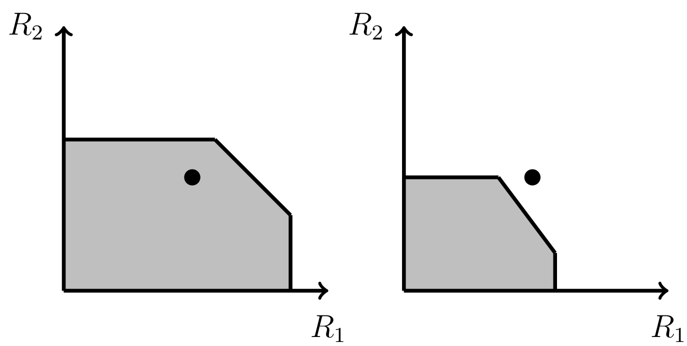


Figure 4.1: Two-user Gaussian MAC capacity regions for different fading realizations along with a specific rate pair marked with a circle.

## 4.2 Optimal Rate Selection

In this section, we extend our approach in the previous chapter to systems with a (common) receiver with MUD capabilities. We assume that the MUD capability is limited to the collisions of two packets as this is more practical, and explicit and implementable codes exist [27].

### 4.2.1 Problem Definition and Solution

We model each collision as a Gaussian MAC with fading, and denote the rate of user $i$ by $R_i$ where $i = 1, 2, \ldots, n$. We note that optimal rates $R_i$'s are the functions of all the distances of the users which are assumed as known.[1] For the expected throughput formulation, we modify (3.4) with the addition of decodable two-user collisions. Therefore, in the formulation, there is a summation of $n$ terms for single level decoding which occurs if there is only one user active in a slot, and there is summation of $\binom{n}{2}$ additional terms for two-level decoding (which means that the decoder may be successful when at most two packets collide). For each of these $\binom{n}{2}$ terms, there are three inequalities specified in (4.1) for two-user

[1]It is a function of the distance of the particular user only in the single user detection case.

Gaussian MAC capacity determining whether the decoding is successful or there is a decoder failure.

Similarly, for $m$-level decoding, there are $\binom{n}{m}$ additional terms and for each of them $(2^m - 1)$ additional inequalities are needed compared to the $(m-1)$-level decoding. Hence, the formulation here can be easily extended, however, the calculations needed for the optimization will be more cumbersome. Also, we exclude the cases where one of the two users can be decoded by treating the other as noise (i.e., we assume the users are either both decodable or both undecodable in a collision).

The expected throughput in (3.4) can then be written as

$$T = \sum_{i=1}^{n} R_i \mathbf{P}(R_i < C(P_i h_i^2)) p_i \prod_{\substack{j=1 \\ j\neq i}}^{n} (1-p_j) + \sum_{i=1}^{n} p_i \sum_{j=i+1}^{n} p_j \prod_{\substack{k=1 \\ k\neq i,j}}^{n} (1-p_k)(R_i+R_j)$$
$$\mathbf{P}\Big(R_i < C(P_i h_i^2), R_j < C(P_j h_j^2), (R_i+R_j) < C((P_i h_i^2) + (P_j h_j^2))\Big). \tag{4.2}$$

We define the two-user non-outage probability as $A(R_i, R_j)$, and denote $Nd_i^{\gamma}/P_0$ by $\alpha_i$. Since $h_i^2, h_j^2$ are independent and identically distributed (*i.i.d.*) exponential random variables, for $\alpha_i \neq \alpha_j$, we can write

$$\begin{aligned}
A(R_i, R_j) =& \mathbf{P}\Big(R_i < C(P_i h_i^2), R_j < C(P_j h_j^2), (R_i+R_j) < C((P_i h_i^2) + (P_j h_j^2))\Big) \\
=& \mathbf{P}(\gamma_i \geq 2^{2R_i} - 1, \gamma_j \geq 2^{2R_j} - 1, \gamma_i + \gamma_j \geq 2^{2(R_i+R_j)} - 1) \\
=& \int_{2^{2R_i}-1}^{\infty} f_{\gamma_i}(x) \mathbf{P}(\gamma_j \geq \max(2^{2R_j} - 1, 2^{2(R_i+R_j)} - 1 - x)) \mathrm{d}x \\
=& \int_{2^{2R_i}-1}^{2^{2R_j}(2^{2R_i}-1)} f_{\gamma_i}(x) \int_{2^{2(R_i+R_j)}-1-x}^{\infty} f_{\gamma_j}(y) \mathrm{d}y \mathrm{d}x \\
&+ \int_{2^{2R_j}(2^{2R_i}-1)}^{\infty} f_{\gamma_i}(x) \int_{2^{2(R_j)}-1}^{\infty} f_{\gamma_j}(y) \mathrm{d}y \mathrm{d}x \\
=& \int_{2^{2R_i}-1}^{2^{2R_j}(2^{2R_i}-1)} \alpha_i e^{-\alpha_i x} e^{-\alpha_j (2^{2(R_i+R_j)}-1-x)} \mathrm{d}x \\
&+ \exp(-\alpha_j (2^{2R_j} - 1)) \exp(-\alpha_i (2^{2R_i} - 1) 2^{2R_j})
\end{aligned} \tag{4.3}$$

where $\gamma_i = P_i h_i^2/N$ and $f_{\gamma_i}(x)$ denotes the probability density function of $\gamma_i$.

Then, we have

$$\begin{aligned}A(R_i, R_j) =& \frac{\alpha_i}{\alpha_j - \alpha_i} \exp(-\alpha_j(2^{2(R_i+R_j)} - 1))\Big( \exp((\alpha_j - \alpha_i)(2^{2R_i} - 1)2^{2R_j})- \\ & \exp((\alpha_j - \alpha_i)(2^{2R_i} - 1))\Big) + \exp(-\alpha_j(2^{2R_j} - 1)) \exp(-\alpha_i(2^{2R_i} - 1)2^{2R_j}).\end{aligned} \tag{4.4}$$

For the case with $\alpha_i = \alpha_j$, the two-user non-outage probability can be written as

$$\begin{aligned}A(R_i, R_j) =& \mathbf{P}\Big(R_i < C(P_i h_i^2), R_j < C(P_j h_j^2), (R_i + R_j) < C((P_i h_i^2) + (P_j h_j^2))\Big) \\ =& \mathbf{P}(\gamma_i \geq 2^{2R_i} - 1, \gamma_j \geq 2^{2R_j} - 1, \gamma_i + \gamma_j \geq 2^{2(R_i+R_j)} - 1) \\ =& \int_{2^{2R_i}-1}^{\infty} f_{\gamma_i}(x)\mathbf{P}(\gamma_j \geq \max(2^{2R_j} - 1, 2^{2(R_i+R_j)} - 1 - x))\mathrm{d}x \\ =& \int_{2^{2R_i}-1}^{2^{2R_j}(2^{2R_i}-1)} f_{\gamma_i}(x) \int_{2^{2(R_i+R_j)}-1-x}^{\infty} f_{\gamma_j}(y)\mathrm{d}y\mathrm{d}x \\ & + \int_{2^{2R_j}(2^{2R_i}-1)}^{\infty} f_{\gamma_i}(x) \int_{2^{2(R_j)}-1}^{\infty} f_{\gamma_j}(y)\mathrm{d}y\mathrm{d}x \\ =& \int_{2^{2R_i}-1}^{2^{2R_j}(2^{2R_i}-1)} \alpha_i e^{-\alpha_i(2^{2(R_i+R_j)}-1)}\mathrm{d}x + \exp(-\alpha_i(2^{2(R_i+R_j)} - 1).\end{aligned} \tag{4.5}$$

We can simplify this expression as

$$A(R_i, R_j) = (\alpha_i(2^{2R_i} - 1)(2^{2R_j} - 1) + 1) \exp(-\alpha_i(2^{2(R_i+R_j)} - 1)). \tag{4.6}$$

By combining (3.6), (4.2), (4.4) and (4.6), the optimization problem for the rate selection becomes

$$\begin{aligned}\max_{R_1,R_2,\ldots,R_n} &\sum_{i=1}^{n} p_i \prod_{\substack{j=1\\ j\neq i}}^{n} (1-p_j) R_i \exp(-\alpha_i(2^{2R_i}-1)) \\ &+ \sum_{i=1}^{n} p_i \sum_{j=i+1}^{n} p_j \prod_{\substack{k=1\\ k\neq i,j}}^{n} (1-p_k)(R_i+R_j)A(R_i,R_j).\end{aligned} \tag{4.7}$$

Using this formulation, given the activity probabilities $p_i$'s and the distance of the users $d_i$'s, the optimal rates $R_i^*$'s can be found via numerical tools such as gradient descent algorithms or interior-point methods[2]. We also note that some optimal rates can be zero as the sole objective is the overall throughput maximization.

### 4.2.2 Analysis of the Solution

To analyze the global optimality of the solution, we modify the optimization problem to obtain a relaxed version of it by using an upper bound on the two-user MAC capacity, and we guarantee that the solution of this modified problem converges to a globally optimal point.

For simplicity, we use an upper bound on the MAC capacity region defined by $R_i + R_j < C(P_i h_i^2 + P_j h_j^2)$. By using this upper bound for the case of $\alpha_i \neq \alpha_j$, the new non-outage capacity becomes

$$\begin{aligned}\bar{A}(R_i,R_j) =& \mathbf{P}\Big((R_i+R_j) < C((P_i h_i^2) + (P_j h_j^2))\Big) \\ =& \mathbf{P}(\gamma_i + \gamma_j \geq 2^{2(R_i+R_j)} - 1) \\ =& \int_0^{2^{2(R_i+R_j)}-1} f_{\gamma_i}(x) \int_{2^{2(R_i+R_j)}-1-x}^{\infty} f_{\gamma_j}(y)\mathrm{d}y\mathrm{d}x + \int_{2^{2(R_i+R_j)}-1}^{\infty} f_{\gamma_i}(x)\mathrm{d}x \\ =& \int_0^{2^{2(R_i+R_j)}-1} \alpha_i e^{-\alpha_i x} e^{-\alpha_j (2^{2(R_i+R_j)}-1-x)}\mathrm{d}x + \exp(-\alpha_i(2^{2(R_i+R_j)}-1)),\end{aligned} \tag{4.8}$$

[2]The details of these techniques are not provided in this thesis, and can be found in [36].

which can be evaluated as

$$\bar{A}(R_i, R_j) = \frac{\alpha_j e^{(-\alpha_i(2^{2(R_i+R_j)}-1))}}{\alpha_j - \alpha_i} - \frac{\alpha_i e^{(-\alpha_j(2^{2(R_i+R_j)}-1))}}{\alpha_j - \alpha_i}. \tag{4.9}$$

For the case of $\alpha_i = \alpha_j$, the new non outage capacity can be written as

$$\begin{aligned}\bar{A}(R_i, R_j) =& \mathbf{P}\Big((R_i + R_j) < C((P_i h_i^2) + (P_j h_j^2))\Big)\\ =& \mathbf{P}(\gamma_i + \gamma_j \geq 2^{2(R_i+R_j)} - 1)\\ =& \int_0^{2^{2(R_i+R_j)}-1} f_{\gamma_i}(x) \int_{2^{2(R_i+R_j)}-1-x}^{\infty} f_{\gamma_j}(y)\mathrm{d}y\mathrm{d}x + \int_{2^{2(R_i+R_j)}-1}^{\infty} f_{\gamma_i}(x)\mathrm{d}x\\ =& \int_0^{2^{2(R_i+R_j)}-1} \alpha_i e^{-\alpha_i(2^{2(R_i+R_j)}-1)}\mathrm{d}x + \exp(-\alpha_i(2^{2(R_i+R_j)} - 1)),\end{aligned} \tag{4.10}$$

resulting in

$$\bar{A}(R_i, R_j) = (\alpha_i(2^{2(R_i+R_j)} - 1) + 1)\exp(-\alpha_i(2^{2(R_i+R_j)} - 1)). \tag{4.11}$$

We modify the throughput expression in (4.7) by substituting $A(R_i, R_j)$ with the upper bound $\bar{A}(R_i, R_j)$. Then, we write the system throughput $\widetilde{T}_{MUD}$ as a summation of single user throughputs $T_i$'s and two-user collision throughputs $\widetilde{T}_{ij}$'s. Namely,

$$\widetilde{T}_{MUD} = \sum_{i=1}^{n} T_i + \sum_{i=1}^{n} \sum_{j=i+1}^{n} \widetilde{T}_{ij} \tag{4.12}$$

where $T_i = p_i \prod_{\substack{j=1\\ j\neq i}}^{n}(1-p_j)R_i \exp(-\alpha_i(2^{2R_i}-1))$ and $\widetilde{T}_{ij} = p_i p_j \prod_{\substack{k=1\\ k\neq i,j}}^{n}(1-p_k)(R_i+R_j)\bar{A}(R_i, R_j)$.

In the previous chapter, we have proved that the solution obtained for single user throughput $T_i$ is globally optimal. The first derivative of $T_i$ w.r.t. $R_i$ is given in (3.13), and at the optimal rates, we have

$$1 - 2^{2R^*(d_i)}\alpha_i 2R^*(d_i)\ln 2 = 0. \tag{4.13}$$

The second derivative is given by

$$\frac{\partial^2(-T_i)}{\partial R(d_i)^2} = e^{-(2^{2R(d_i)}-1)\alpha_i} p_i \prod_{\substack{j=1\\ j\neq i}}^{n} (1-p_j) 2^{2R(d_i)} 4\alpha_i \ln 2 (1-2^{2R(d_i)}\alpha_i R(d_i) \ln 2 + R(d_i) \ln 2). \tag{4.14}$$

We also have the first derivative of $-\widetilde{T}_{ij}$ as

$$\frac{\partial(-\widetilde{T}_{ij})}{\partial R_i} = p_i p_j \prod_{\substack{k=1\\ k\neq i,j}}^{n} (1-p_k)[\alpha_j e^{-\alpha_i \sigma} - \alpha_i e^{-\alpha_j \sigma} - 2^{2(R_i+R_j)} \alpha_i \alpha_J 2(R_i+R_j) \ln 2 (e^{-\alpha_i \sigma} - e^{-\alpha_j \sigma})] \tag{4.15}$$

where $\sigma = 2^{2(R_i+R_j)} - 1$.

For the second derivative we have

$$\begin{aligned}\frac{\partial^2(-\widetilde{T}_{ij})}{\partial R_i^2} =& \frac{\partial^2(-\widetilde{T}_{ij})}{\partial R_j^2} = \frac{\partial^2(-\widetilde{T}_{ij})}{\partial R_i \partial R_j}\\ =& \frac{-2(\sigma_1 \alpha_i \alpha_j \sigma_3 \ln(2) - \sigma_1 \alpha_i \alpha_j \sigma_2 \ln(2))}{\alpha_i - \alpha_j}\\ &+ \frac{-2^{2(R_i+R_j)+2} \alpha_i \alpha_j \ln(2)^2 (R_i + R_j)(\sigma_3 - \sigma_2 - \sigma_4 \alpha_i \sigma_3 + \sigma_4 \alpha_j \sigma_2)}{\alpha_i - \alpha_j}\end{aligned} \tag{4.16}$$

where $\sigma_1 = 2^{2(R_i+R_j)+1}$, $\sigma_2 = e^{-\alpha_j(\sigma_4 - 1)}$, $\sigma_3 = e^{-\alpha_i(\sigma_4-1)}$ and $\sigma_4 = 2^{2(R_i+R_j)}$.

We can write $n \times n$ Hessian matrix $\mathbf{H}$ of $-\widetilde{T}_{MUD}$ as follows.

$$\mathbf{H} = \begin{bmatrix} \left(\frac{\partial^2(-T_1)}{\partial R_1^2} + \frac{\partial^2(-\widetilde{T}_{12})}{\partial R_1^2} + \cdots + \frac{\partial^2(-\widetilde{T}_{1n})}{\partial R_1^2}\right) & \frac{\partial^2(-\widetilde{T}_{12})}{\partial R_1 \partial R_2} & \cdots & \frac{\partial^2(-\widetilde{T}_{1n})}{\partial R_1 \partial R_n} \\ \frac{\partial^2(-\widetilde{T}_{12})}{\partial R_1 \partial R_2} & & & \\ \vdots & & \ddots & \vdots \\ \frac{\partial^2(-\widetilde{T}_{1n})}{\partial R_1 \partial R_n} & & \cdots & \left(\frac{\partial^2(-T_n)}{\partial R_n^2} + \frac{\partial^2(-\widetilde{T}_{1n})}{\partial R_n^2} + \cdots + \frac{\partial^2(-\widetilde{T}_{2n})}{\partial R_2^2}\right) \end{bmatrix} \tag{4.17}$$

Consider an arbitrary column vector $\mathbf{x}$, and compute

$$\begin{aligned}\mathbf{x}^T\mathbf{H}\mathbf{x} =& x_1^2\left(\frac{\partial^2(-T_1)}{\partial R_1^2}+\frac{\partial^2(-\widetilde{T}_{12})}{\partial R_1^2}+\cdots+\frac{\partial^2(-\widetilde{T}_{1n})}{\partial R_1^2}\right)+x_1x_2\frac{\partial^2(-\widetilde{T}_{12})}{\partial R_1\partial R_2}\\ &+x_1x_3\frac{\partial^2(-\widetilde{T}_{13})}{\partial R_1\partial R_3}+\cdots+x_1x_n\frac{\partial^2(-\widetilde{T}_{1n})}{\partial R_1\partial R_n}\\ &+x_2^2\left(\frac{\partial^2(-T_2)}{\partial R_2^2}+\frac{\partial^2(-\widetilde{T}_{12})}{\partial R_2^2}+\cdots+\frac{\partial^2(-\widetilde{T}_{2n})}{\partial R_2^2}\right)+x_1x_2\frac{\partial^2(-\widetilde{T}_{12})}{\partial R_1\partial R_2}\\ &+x_2x_3\frac{\partial^2(-\widetilde{T}_{23})}{\partial R_2\partial R_3}+\cdots+x_2x_n\frac{\partial^2(-\widetilde{T}_{2n})}{\partial R_2\partial R_n}\\ &\quad\vdots\\ &+x_n^2\left(\frac{\partial^2(-T_n)}{\partial R_n^2}+\frac{\partial^2(-\widetilde{T}_{1n})}{\partial R_n^2}+\cdots+\frac{\partial^2(-\widetilde{T}_{(n-1)n})}{\partial R_n^2}\right)+x_1x_n\frac{\partial^2(-\widetilde{T}_{1n})}{\partial R_1\partial R_2 n}\\ &+x_2x_n\frac{\partial^2(-\widetilde{T}_{2n})}{\partial R_2\partial R_n}+\cdots+x_{n-1}x_n\frac{\partial^2(-\widetilde{T}_{(n-1)n})}{\partial R_{n-1}\partial R_n}.\end{aligned} \tag{4.18}$$

This can be simplified by using (4.16) as

$$\begin{aligned}\mathbf{x}^T\mathbf{H}\mathbf{x} =& \frac{\partial^2(-\widetilde{T}_{12})}{\partial R_1\partial R_2}(x_1+x_2)^2+\frac{\partial^2(-\widetilde{T}_{13})}{\partial R_1\partial R_3}(x_1+x_3)^2+\frac{\partial^2(-\widetilde{T}_{23})}{\partial R_2\partial R_3}(x_2+x_3)^2\\ &+\cdots+\frac{\partial^2(-\widetilde{T}_{nn-1})}{\partial R_{n-1}\partial R_n}(x_n+x_{n-1})^2\\ &+\frac{\partial^2(-T_1)}{\partial R_1^2}x_1^2+\frac{\partial^2(-T_2)}{\partial R_2^2}x_2^2+\cdots+\frac{\partial^2(-T_n)}{\partial R_n^2}x_n^2.\end{aligned} \tag{4.19}$$

Clearly, if $\frac{\partial^2(-T_i)}{\partial R_i^2}\geq 0$ and $\frac{\partial^2(-\widetilde{T}_{ij})}{\partial R_i^2}\geq 0$ for $i=1,2,\ldots,n$, then $\mathbf{x}^T\mathbf{H}\mathbf{x}\geq 0$, therefore the matrix $\mathbf{H}$ is positive semi-definite, and $-\widetilde{T}_{MUD}$ is convex and $\widetilde{T}_{MUD}$ is concave.

Then, $T_i$ is concave in the domain $[0, M_i]$ since $\frac{\partial^2(-T_i)}{\partial R_i^2}\geq 0$ for $R_i < M_i$ where $M_i$ is a constant. By using (4.13) and the inequality $(1-2^{2R_i}\alpha_i R_i\ln 2+R_i\ln 2)\geq 0$ from (4.14) for concavity, we obtain

$$1/2+R^*(d_i)\ln 2\geq 0. \tag{4.20}$$

Hence, our optimal solution in (3.10) is inside the concavity domain $[0, M_i]$.

From (4.16) and assuming $\alpha_j > \alpha_i$, for concavity, we also have

$$(e^{-\alpha_i\sigma} - e^{-\alpha_j\sigma}) + \ln 2(R_i + R_j)[(e^{-\alpha_i\sigma} - e^{-\alpha_j\sigma}) - \alpha_i e^{-\alpha_i\sigma} 2^{2(R_i+R_j)} + \alpha_j e^{-\alpha_j\sigma} 2^{2(R_i+R_j)}] \geq 0. \quad (4.21)$$

Note that (4.21) holds for $R_i + R_j < M_{ij}$ where $M_{ij}$ is a constant.

Now, we investigate whether single user rates are in this domain $[0, M_{ij}]$. From (3.10), we have $2^{2(R_i+R_j)} = \frac{1}{\alpha_i\alpha_j W(1/\alpha_i)W(1/\alpha_j)}$. By denoting $C = W(1/\alpha_i)W(1/\alpha_j)$, we can write

$$C(e^{-\alpha_i\sigma} - e^{-\alpha_j\sigma}) + \ln 2(R_i + R_j)[\frac{\alpha_j C - 1}{\alpha_j} e^{-\alpha_i\sigma} - \frac{\alpha_i C - 1}{\alpha_i} e^{-\alpha_j\sigma}] \geq 0. \quad (4.22)$$

Then, we obtain

$$(C - \frac{1}{\alpha_j})e^{-\alpha_i\sigma} - (C - \frac{1}{\alpha_i})e^{-\alpha_j\sigma} \geq 0. \quad (4.23)$$

Finally, since $(C - \frac{1}{\alpha_j}) > (C - \frac{1}{\alpha_i})$ and $e^{-\alpha_i\sigma} > e^{-\alpha_j\sigma}$, (4.23) holds, and the single user optimal rates $R_i^*$ and $R_j^*$ are inside this concavity domain.

Since the optimal rates are inside both domains $[0, M_i]$ and $[0, M_{ij}]$, our problem becomes convex in the domain $(R_i, R_j) \in [0, R_i^*] \times [0, R_j^*]$. Fig. 4.2 shows an illustration of these regions.

We know that the optimal rates with MUD are upper bounded by the single user rates $R_i^*$ and $R_j^*$ due to the fact that capacity region of two-user channel is inside of the union of the single user regions. Therefore by using the constraints $R_i \leq \frac{W\left(\frac{P_0}{N d_i^\gamma}\right)}{\ln(4)}$ for $i = 1, 2, \ldots, n$, we can guarantee that an iterative optimization algorithm converges to the globally optimum solution for the relaxed version of the original problem.

Via extensive numerical examples, we have observed that the solution of the modified problem closely matches with the solution of the original problem. Therefore, we can argue that the algorithm that we use to solve the original

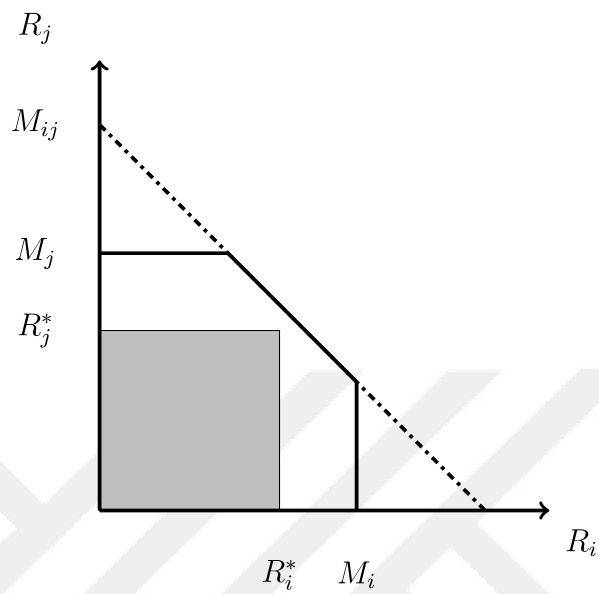


Figure 4.2: Shaded region is the new constraint to guarantee a convex set of constraints in the optimization problem.

rate selection problem converges to a point close to the globally optimal one (at least for the numerical examples considered).

## 4.3 System Design with Fairness

In highly asymmetric scenarios where some of the users are much closer to the destination than the others, the individual throughputs of far away users become very low compared to the closer users. With this motivation, we now consider the extension of the proposed scheme for the case with MUD by also taking into account fairness among the users. Specifically, we propose a method to compute the optimal rates and activity probabilities.

### 4.3.1 Problem Definition and Solution

The optimization problem in this case can be formulated as

$$
\begin{aligned}
\max_{\substack{p_1,p_2,\ldots,p_n\\R_1,R_2,\ldots,R_n}} \; & \sum_{i=1}^{n} p_i \prod_{\substack{j=1\\j\neq i}}^{n} (1-p_j) R_i \exp(-\alpha_i(2^{2R_i}-1)) \\
& + \sum_{i=1}^{n} p_i \sum_{j=i+1}^{n} p_j \prod_{\substack{k=1\\k\neq i,j}}^{n} (1-p_k)(R_i+R_j)A(R_i,R_j) \\
\text{s.t.} \quad & R_i \Bigg( p_i \prod_{\substack{j=1\\j\neq i}}^{n} (1-p_j) \exp(-\alpha_i(2^{2R_i}-1)) \\
& + p_i \sum_{\substack{j=1\\j\neq i}}^{n} p_j \prod_{\substack{k=1\\k\neq i,j}}^{n} (1-p_k) A(R_i,R_j) \Bigg) \geq K \\
& 0 \leq p_i \leq 1, \quad \text{for} \quad i = 1,2,\ldots,n.
\end{aligned}
\tag{4.24}
$$

where $K$ is the minimum throughput required for each user. The optimal rates $R_i^*$ and activity probabilities $p_i^*$ can then be determined via the following steps:

1. Set the initial values for $R_i$'s.
2. Fix $R_i$'s and find the optimal $p_i^*$'s with an interior-point method, and update $p_i$'s with the newly found values.
3. Fix $p_i$'s and find the optimal $R_i^*$'s with an interior-point method and update $R_i$'s with the newly found $R_i^*$'s. Calculate $T_{fair}^*$ with the current values of $p_i$'s and $R_i$'s.
4. Examine whether $T_{fair}^* - T_{fair}$ is higher than some small tolerance $\epsilon$. If so, return to step 2 and update $T_{fair}$ with $T_{fair}^*$. If not, stop and (set as the optimal rates and activity probabilities $R_i$ and $p_i$, respectively).

This method is guaranteed to converge, however, the solution may be a locally optimal one. This is because the objective function increases after each iteration, and it is bounded from above. It can also be noted that, the optimal rates and activity probabilities can be found jointly in one step, however, the proposed step by step approach helps reduce the complexity and is more practical.

## 4.4 Limiting Individual Outage Probabilities

Similar to the case where MUD is not performed at the receiver side (discussed in Section 3.4), we also consider limiting the individual outage probabilities for the present scheme. By limiting outage, we can decrease the delay caused by retransmissions, and we can potentially increase the energy efficiency of the system. We note that, in this section, we focus on the outage cases only (without calculating total delay or energy consumption).

We formulate the corresponding optimization problem as

$$\begin{aligned}
\max_{R_1,R_2,\ldots,R_n} & \sum_{i=1}^{n} p_i \prod_{\substack{j=1\\ j\neq i}}^{n} (1-p_j) R_i \exp(-\alpha_i(2^{2R_i}-1)) \\
& + \sum_{i=1}^{n} p_i \sum_{j=i+1}^{n} p_j \prod_{\substack{k=1\\ k\neq i,j}}^{n} (1-p_k)(R_i+R_j) A(R_i,R_j) \qquad (4.25)\\
\text{s.t.} \quad & 1-\exp(-\alpha_i(2^{2R_i}-1)) \leq \beta_i \\
& 1 - A(R_i,R_j) \leq \beta_i, \quad \forall j \\
& 0 \leq p_i \leq 1, \quad \text{for} \quad i = 1,2,\ldots,n.
\end{aligned}$$

where $\beta_i$ is the maximum allowed individual outage probability for each user. Given feasible $\beta_i$'s and the activity probabilities $p_i$'s, the optimal rates $R_i^*$'s can be found via numerical algorithms such as gradient descent or interior-point methods.

## 4.5 Effects of Shadowing

In this section, we investigate the effects of shadowing on rate selection. As discussed in Section 3.5 for the single user case, modification occurs only in the outage probability formulation of the mathematical model used for the optimal rate selection problem. For simplicity, for the MUD case, we ignore Rayleigh fading and assume that log-normal shadowing is the only source of channel variation along with the path-loss. Therefore, in this case the SNR becomes $P_i\Psi_i/N$ for user $i$ where $\Psi_i$ is a log-normal random variable with parameters $\mu = 0$ and $\sigma^2$. We can then modify the non-outage expression in (4.3) as

$$\begin{aligned}
A(R_i, R_j) =& \mathbf{P}\Big(R_i < C(P_i\Psi_i), R_j < C(P_j\Psi_j), (R_i + R_j) < C((P_i\Psi_i) + (P_j\Psi_j))\Big) \\
=& \mathbf{P}(\gamma_i \geq 2^{2R_i} - 1, \gamma_j \geq 2^{2R_j} - 1, \gamma_i + \gamma_j \geq 2^{2(R_i+R_j)} - 1) \\
=& \int_{2^{2R_i}-1}^{\infty} f_{\gamma_i}(x)\mathbf{P}(\gamma_j \geq \max(2^{2R_j} - 1, 2^{2(R_i+R_j)} - 1 - x))\mathrm{d}x \\
=& \int_{2^{2R_i}-1}^{2^{2R_j}(2^{2R_i}-1)} f_{\gamma_i}(x) \int_{2^{2(R_i+R_j)}-1-x}^{\infty} f_{\gamma_j}(y)\mathrm{d}y\mathrm{d}x \\
&+ \int_{2^{2R_j}(2^{2R_i}-1)}^{\infty} f_{\gamma_i}(x) \int_{2^{2(R_j)}-1}^{\infty} f_{\gamma_j}(y)\mathrm{d}y\mathrm{d}x \\
=& \int_{2^{2R_i}-1}^{2^{2R_j}(2^{2R_i}-1)} \frac{1}{\alpha_i x\sigma\sqrt{2\pi}} \exp\left(-\frac{(\ln(\alpha_i x))^2}{2\sigma^2}\right) \\
&\left(\frac{1}{2} - \frac{1}{2}\mathrm{erf}(\frac{\ln(\alpha_j(2^{2(R_i+R_j)} - 1 - x))}{\sqrt{2}\sigma})\right)\mathrm{d}x \\
&+ \left(\frac{1}{2} - \frac{1}{2}\mathrm{erf}(\frac{\ln(\alpha_i 2^{2R_j}(2^{2R_i} - 1)}{\sqrt{2}\sigma})\right)\left(\frac{1}{2} - \frac{1}{2}\mathrm{erf}(\frac{\ln(\alpha_j(2^{2R_j} - 1))}{\sqrt{2}\sigma})\right).
\end{aligned} \tag{4.26}$$

Since the above expression is not easy to manipulate, we proceed with numerical tools for its evaluation and computation of the optimal rates $R_1, R_2, \ldots, R_n$. In order to compute the optimal rates, we use both the single user non-outage probability in (3.34) and the multi-user non-outage probability in (4.26) since single user transmissions are also possible in each slot.

## 4.6 Numerical Examples

### 4.6.1 Optimal Rate Selection

To illustrate the optimal rate selection in a slotted ALOHA with MUD, we consider a 5-user setup where the users are placed at different distances from the common receiver[3]. We set the average SNR to 17 dB and the path-loss exponent $\gamma$ to 3. Fig. 4.3 shows the resulting optimal rates of the users in the symmetric scenario of equal activity probabilities. Optimal rates in the asymmetric scenarios can also be found similarly as the framework adopted in (4.7) is general.

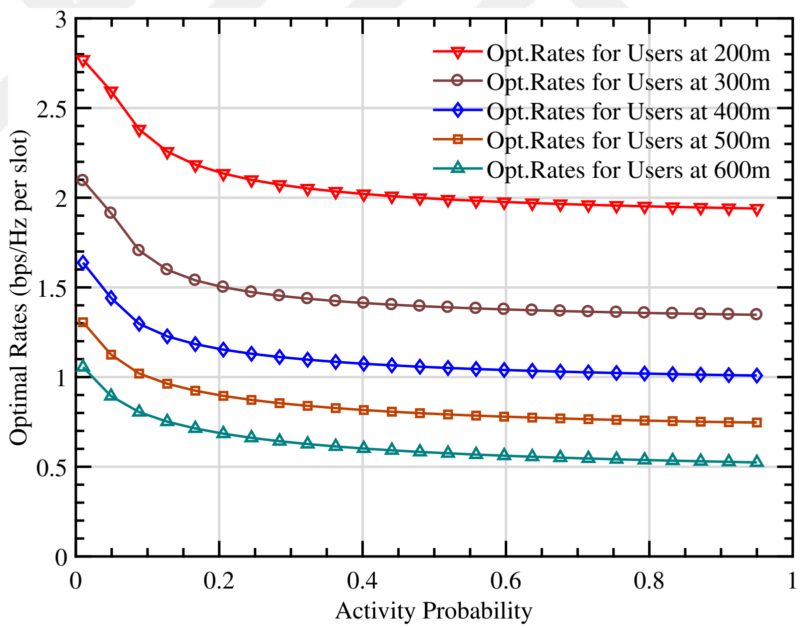


Figure 4.3: Optimal rates for 5-user setup in MUD case.

Comparisons between the throughput performances of our model and the model in which same rate is assigned to all the users are presented in Fig. 4.4 for both classical slotted ALOHA setup and slotted ALOHA with MUD. In this example, the users are placed $200m$ to $600m$ away from the receiver. The newly

[3]Note that this is done for clarity of exposition; the method applies equally to scenarios with a large number of users distributed over a geographical area each with a low activation probability in each slot.

proposed method outperforms the results of the same rate assumption by 18% for the both cases with MUD and without MUD. We also note that, if the users are more spatially separated, the gains increase further.

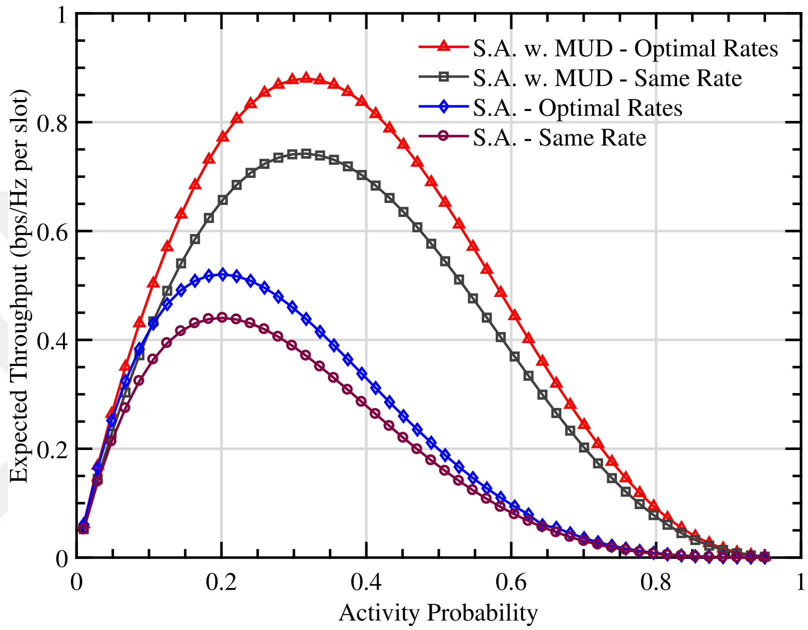


Figure 4.4: Expected throughput vs. activity probabilities

In the provided method to find the optimal rates, we assume that the distances of users are known which may lead to a high-complexity receiver. This is because the optimization process should be repeated for each update on the distances, and receiver should use a feedback link to notify the users after these updates about the new optimal rates. To reduce the receiver complexity and eliminate this feedback link, optimization process can be applied by using only the statistics of the locations of users. Fig. 4.5 illustrates the optimal rates w.r.t. the distances of the users in a crowded network with low activity probabilities where we set $n = 100$ and $p_1 = p_2 = \ldots = p_n = 0.01$. This type of a network is more realistic for the applications of M2M communications and IoT. The receiver can obtain a rate selection curve as in Fig. 4.5 without knowing the exact distances (but using the uniform distribution of them for this specific example), and the users can choose their rates using this function with their own distances only.

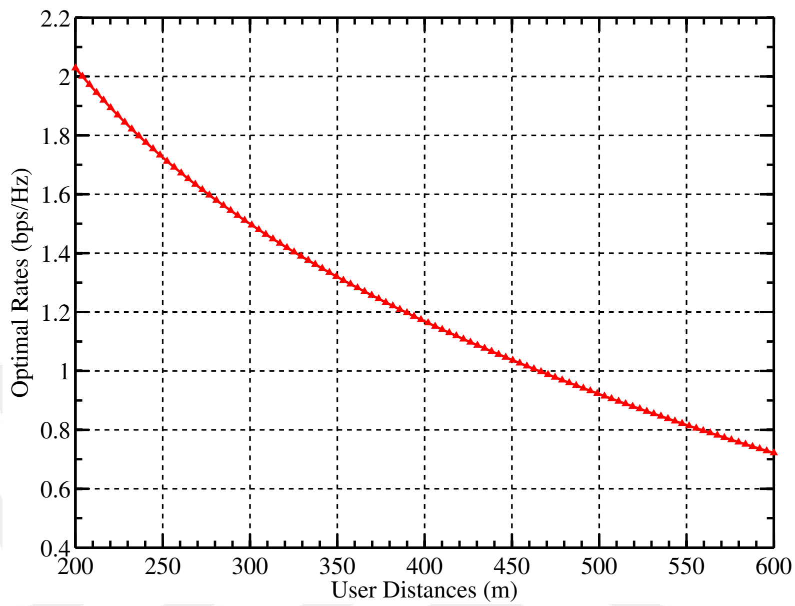


Figure 4.5: Optimal rates vs. user distances where the users are located uniformly between $d_{min} = 200m$ and $d_{max} = 600m$ (with $\gamma$=3 and average SNR=8.7 dB.)

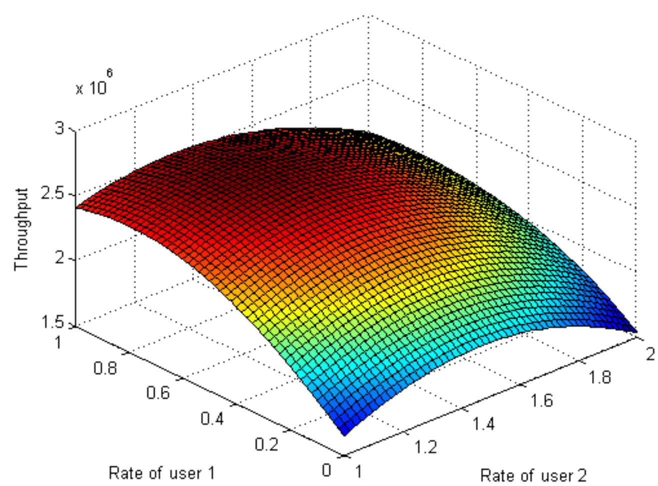


Figure 4.6: Throughput vs. different rate pairs for $d_1 = 300m$ and $d_2 = 200m$.

In order to show the importance of the rate selection on the throughput, Fig. 4.6 and Fig. 4.7 illustrate a two-user setup for $d_1 = 300m$ and $d_2 = 200m$. For a setup with $p_1 = p_2 = 0.2$ and 10 million different realizations of the fading for each rate pair selection, the results are shown for $50 \times 50$ different rate pairs. The efficiency of the optimal rate selection algorithm is evident from the figure. Note that Fig. 4.7 is simply the contour representation of Fig. 4.6.

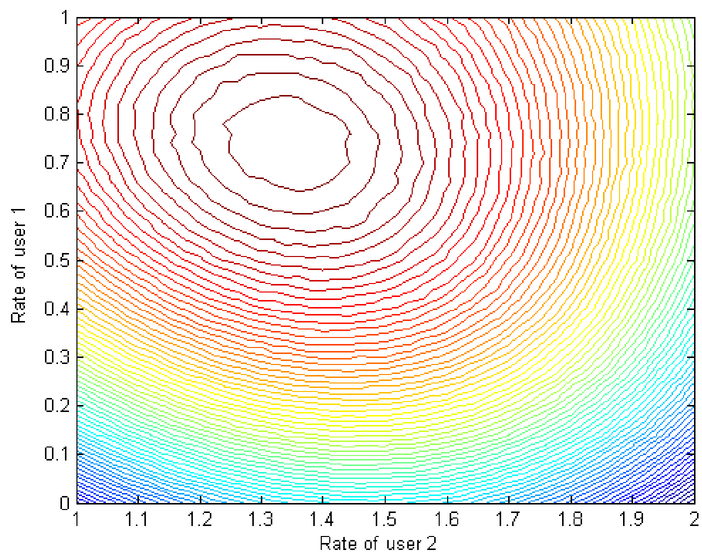


Figure 4.7: Contour of Throughput vs. different rate pairs for $d_1 = 300m$ and $d_2 = 200m$.

### 4.6.2 System Design with Fairness

In this part, we provide examples for the fairness of system with MUD. We use the method described in Section 4.3.1 and the same setup as in Fig. 4.3 and Fig. 4.4 for comparison purposes. That is, we have 5 users with distances 200m, 300m, 400m, 500m and 600m where user 1 is the closest one.

In the first example, we set minimum individual throughput threshold $K = 0.15$. As shown in Fig. 4.8, the system assigns higher activity probabilities to the far away users to maintain the minimum individual throughput. After satisfying the minimum throughput constraints, it is optimal to favor the closest user since it has the largest SNR.

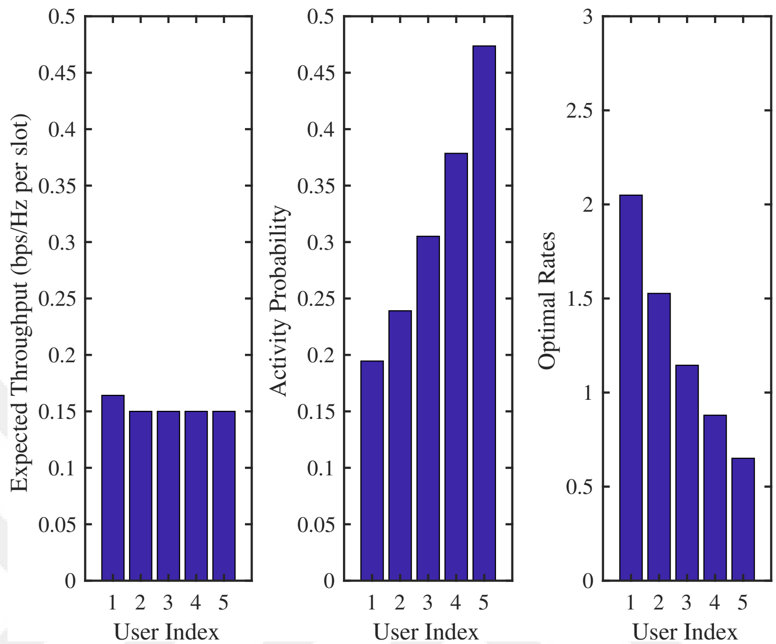


Figure 4.8: A simulation of a fair system with MUD for $K = 0.15$ (with $\gamma = 3$, $d_1 = 200m$, $d_2 = 300m$, $d_3 = 400m$, $d_4 = 500m$, $d_5 = 600m$, $\gamma = 3$, average SNR $= 8.7$ dB).

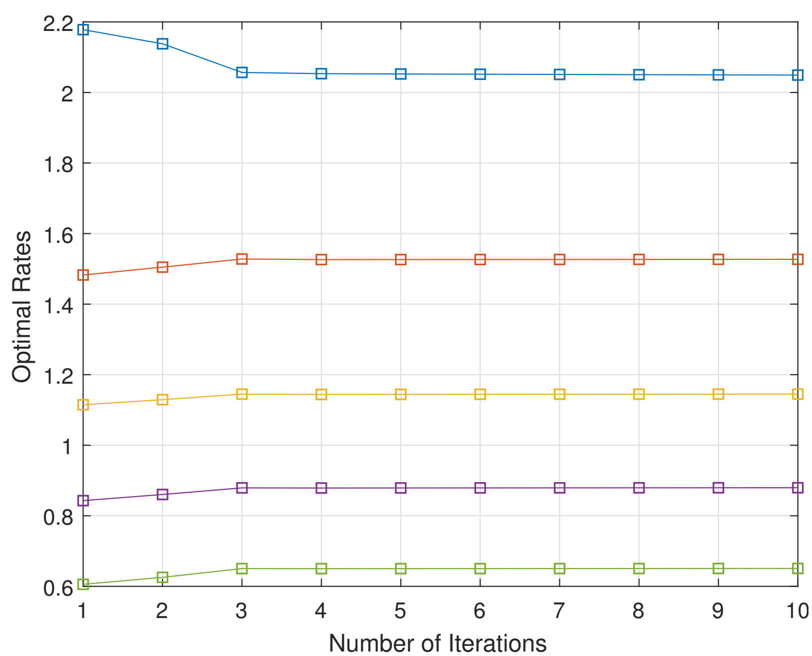


Figure 4.9: Optimal rates vs. number of iterations (with $\gamma = 3$, $d_1 = 200m$, $d_2 = 300m$, $d_3 = 400m$, $d_4 = 500m$, $d_5 = 600m$, average SNR $= 8.7$ dB).

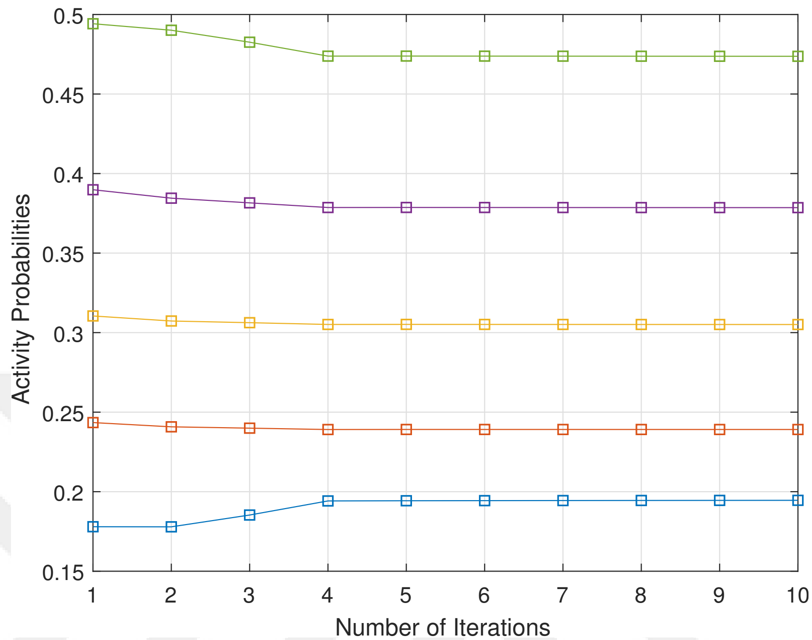


Figure 4.10: Optimal activity probabilities vs. number of iterations (with $\gamma = 3$, $d_1 = 200m$, $d_2 = 300m$, $d_3 = 400m$, $d_4 = 500m$, $d_5 = 600m$, average SNR = 8.7 dB).

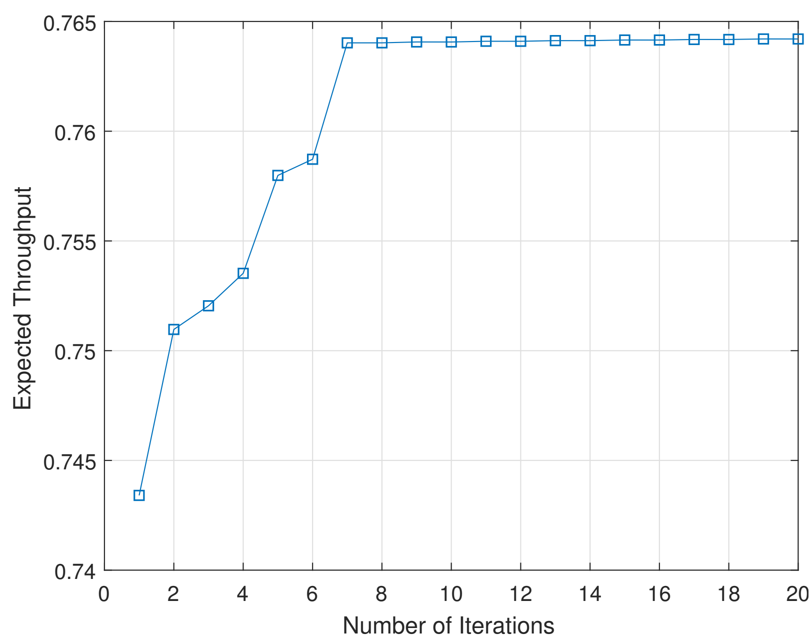


Figure 4.11: System throughput vs. number of iterations (with $\gamma = 3$, $d_1 = 200m$, $d_2 = 300m$, $d_3 = 400m$, $d_4 = 500m$, $d_5 = 600m$, average SNR = 8.7 dB).

To illustrate the change of the optimal rates, activity probabilities and system throughput in each iteration, we present Fig. 4.9, Fig. 4.10 and Fig. 4.11, respectively. We note that same setup is considered with Fig. 4.8, and the optimal rates and activity probabilities we present in Fig. 4.8 are the final iterations of the Fig. 4.9, Fig. 4.10 and Fig. 4.11. We also present the results for minimum individual throughput threshold $K = 0.12$ and $K = 0.10$ in Fig. 4.12 and Fig. 4.13, respectively. Different from the cases where MUD capabilities are not available at the receiver, rate selection has effects on throughput fairness, and the optimal rates vary according to the threshold value $K$ as shown in the figures.

Our results indicate that the optimal activity probabilities increase as $K$ increases for all the users except for the closest one. This result is similar to the single user case. In addition, the optimal rates change according to the change of activity probabilities since they effect each other in the MUD case in a different way compared to the single user setup.

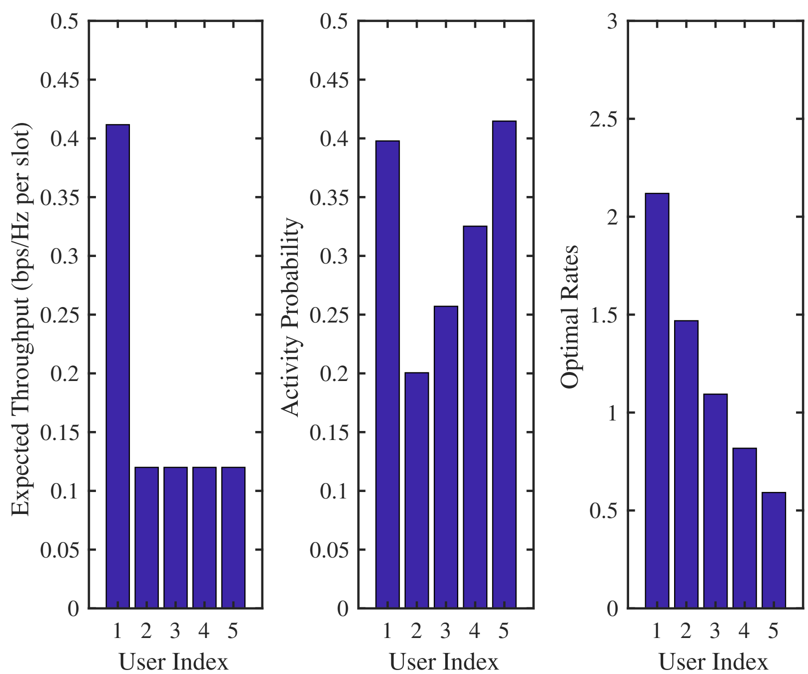


Figure 4.12: A simulation of a fair system with MUD for $K = 0.12$ (with $\gamma = 3$, $d_1 = 200m$, $d_2 = 300m$, $d_3 = 400m$, $d_4 = 500m$, $d_5 = 600m$, $\gamma = 3$, average SNR $= 8.7$ dB).

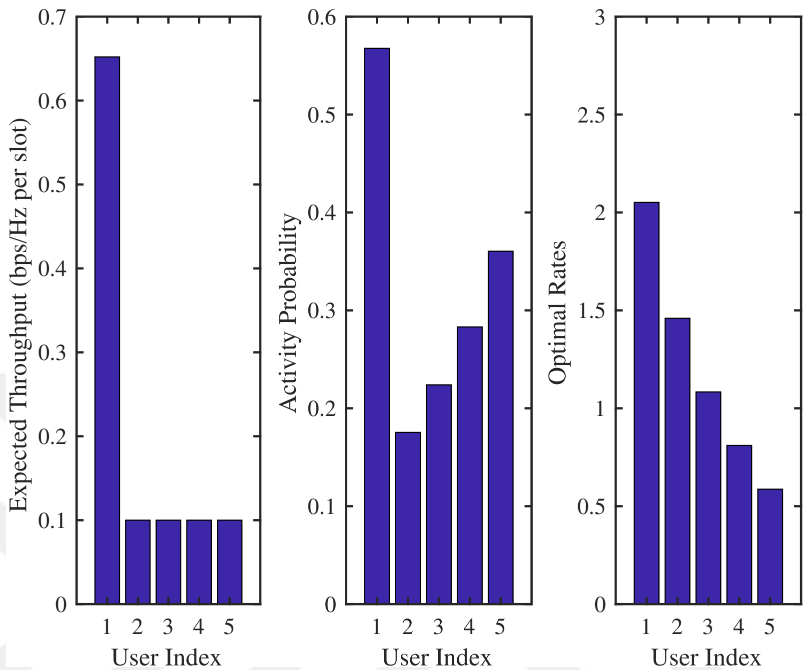

Figure 4.13: A simulation of a fair system with MUD for $K = 0.10$ (with $\gamma = 3$, $d_1 = 200m$, $d_2 = 300m$, $d_3 = 400m$, $d_4 = 500m$, $d_5 = 600m$, $\gamma = 3$, average SNR $= 8.7$ dB).

### 4.6.3 Limiting Outage Probabilities

In this part, we present examples by numerically solving the optimization problem in (4.25), and find optimal rates for the case of limited outage probabilities. We assume a symmetric setup where $\beta_1 = \beta_2 = \ldots = \beta_n = \beta$ for simplicity. We also assume that $p_1 = p_2 = \ldots = p_n = 0.2$. We use the 5-user setup as in Section 4.6.1.

In Fig. 4.14, on the left hand side, we have $\beta = 1$ which means that we do not limit the outage probabilities, while on the right hand side we have $\beta = 0.1$ which means that no outage probability can exceed 0.1. As shown, limiting the outage probabilities decreases the optimal rates. We also present the cases with $\beta = 0.2$ and $\beta = 0.3$ in Fig. 4.15 which demonstrates the same effect.

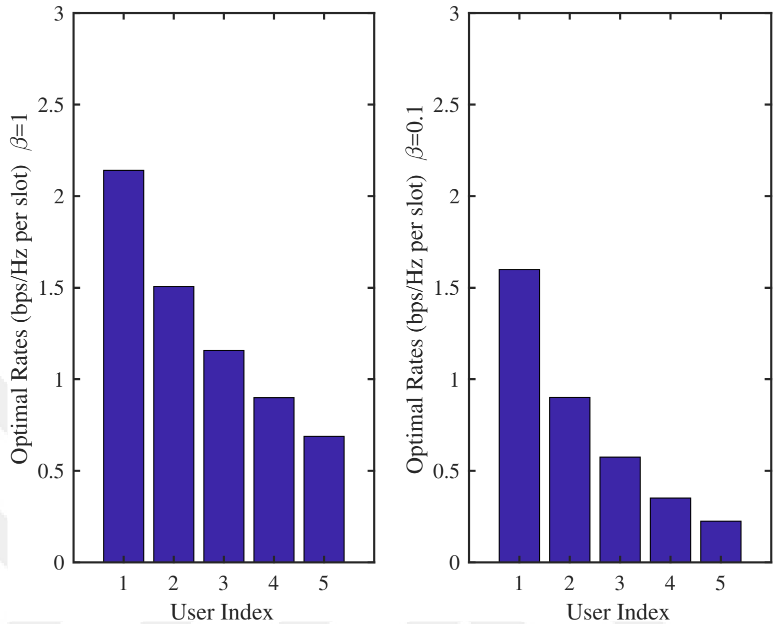


Figure 4.14: System design with limited outage probabilities ($\beta = 1$ for the left hand side plot and $\beta = 0.1$ for the right hand side plot) (with $\gamma = 3$, $d_1 = 200m$, $d_2 = 300m$, $d_3 = 400m$, $d_4 = 500m$, $d_5 = 600m$, $\gamma = 3$, average SNR = 8.7 dB).

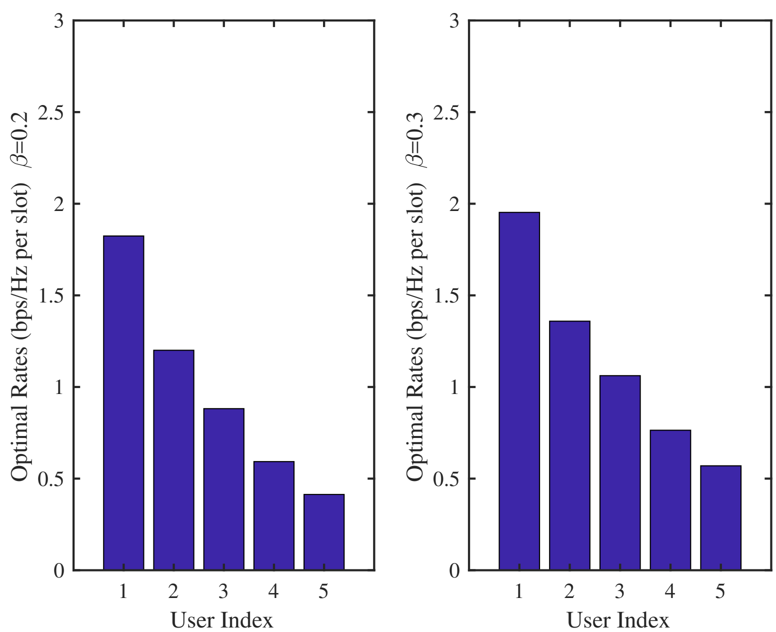


Figure 4.15: System design with limited outage probabilities ($\beta = 0.2$ for the left hand side plot and $\beta = 0.3$ for the right hand side plot) (with $\gamma = 3$, $d_1 = 200m$, $d_2 = 300m$, $d_3 = 400m$, $d_4 = 500m$, $d_5 = 600m$, $\gamma = 3$, average SNR = 8.7 dB).

### 4.6.4 Shadowing Effects

In this part, we investigate the effects of shadowing and make comparisons with the case of Rayleigh fading. Firstly, we present the two-user non-outage probability w.r.t. the selected rates in Fig. 4.16. For the clarity of exposition, we fix the other user's spectral efficiency at 0.8 bps/Hz, $d_1 = 200$ m, $d_2 = 300$ m, and we set $\sigma_{dB} = 3$ or 3.65 dB.

Similar to the single user case, the channel variation increases because of shadowing which causes a slower decrease on the non-outage probability w.r.t. the selected rate. This figure also reveals that shadowing is a more dominant term than fading in terms of the behavior on the non-outage probability when they are both observed in the channel especially for higher $\sigma$ values.

For the same setup as in Fig. 4.16, we also present the expected throughput w.r.t. the selected rate in Fig. 4.17. In these simulations, we specifically focus on the two-user collisions. Also, we note that the throughput is the total throughput of two users. This is the reason for a positive expected throughput at zero rate of this particular user in the figure.

The results indicate that shadowing is destructive for the expected throughput. The reason behind this is that the average SNR is high. As discussed in Section 3.6.4., shadowing has a supportive role at low SNRs, and a destructive role at high SNRs for the single user detection case which appears to be valid for the MUD scenario as well.

The results also show that, shadowing is more dominant than Rayleigh fading on the optimal rates especially with high $\sigma$ values. Hence, our assumption in Section 4.5 where we neglect Rayleigh fading compared to log-normal shadowing for finding the optimal rates seems adequate.

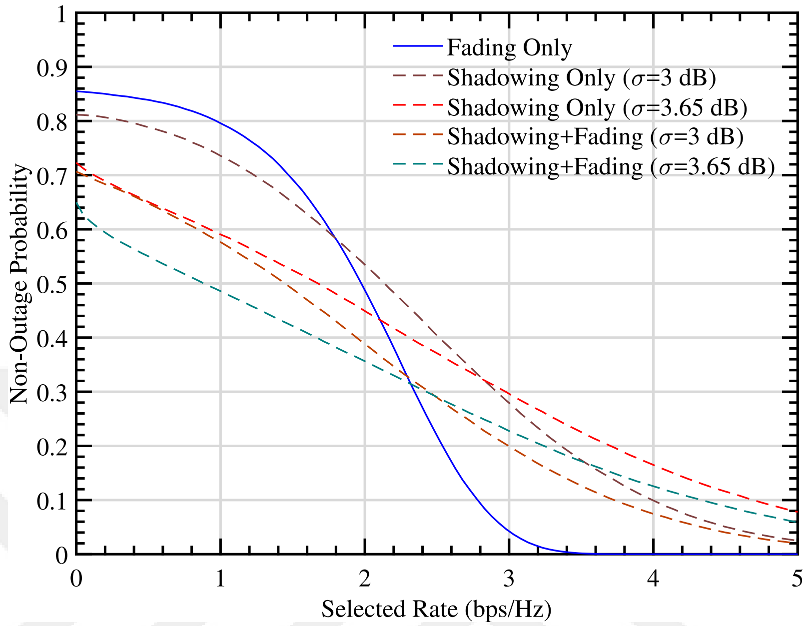


Figure 4.16: Non-outage probability vs. selected rate (with $\gamma = 3.7$, average SNR $= 15.5$ dB).

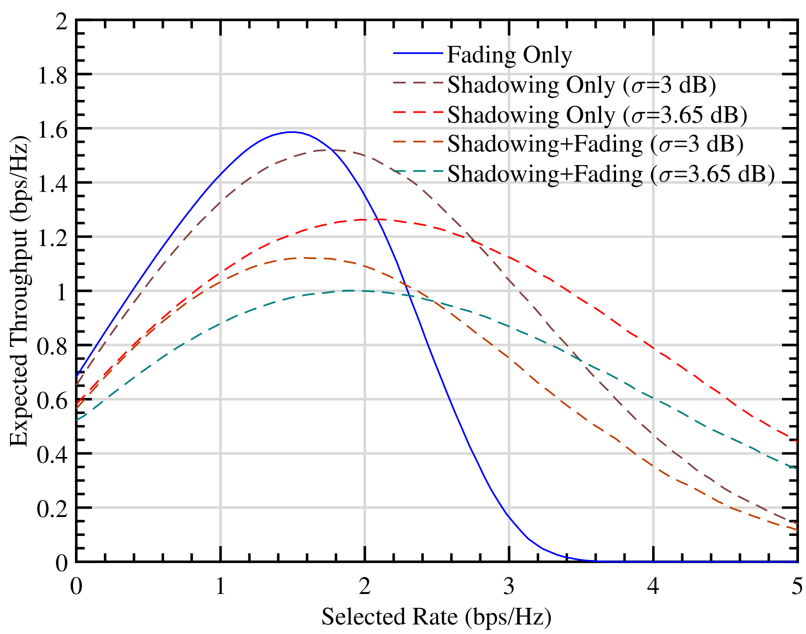


Figure 4.17: Expected throughput vs. selected rate (with $\gamma = 3.7$, average SNR $= 15.5$ dB).

## 4.7 Chapter Summary

In this chapter, we have extended the study of the previous chapter to the case where MUD capability is available at the receiver. We limit the MUD capabilities to two-user collisions, and rather than focusing capacity achieving coding, we focus on the rate selection problem to maximize the system throughput. We examine the individual throughput fairness among different users. We also investigate the limited individual outage probabilities of the transmitters, and design a system under fairness and limited outage probability constraints. In addition, we investigate the effects of shadowing.

Our studies are summarized as follows: We formulate an optimization problem to find the optimal rates, and make the necessary modifications to guarantee that the solution converges to the globally optimal one with simple approaches like gradient descent or interior point methods. The result indicate that an optimal rate selection can be characterized as a function of the all the users' distances to the common receiver and activity probabilities. We observe that the optimal rates are no longer independent of other users' distances and activity probabilities due the induction of MUD capabilities. We also provide a four step method to find the optimal activity probabilities for fairness. Furthermore, we solve the problem with limiting outage probability constraints, and compare the effects of shadowing with Rayleigh fading on the rate selection problem.

# Chapter 5

# Conclusions and Future Work

In this thesis, we have studied the optimal rate and activity selection in random access networks over wireless channels.

The classical slotted ALOHA setup without any MUD capabilities at the receiver is considered. The optimal rate selection problem with Rayleigh fading is solved. The results are in the form of a closed-form rate selection function for each user which depends on the particular user's distance to the common receiver. We then have investigated individual throughput of users and designed systems with throughput fairness by allowing the far away users to send their packets more frequently. To this end, we have characterized the optimal activity probabilities in closed-form. We have also considered individual outage probabilities and designed systems with limited outage for energy efficiency and reduced delay. We find a closed-form optimal rate for this formulation as well. In addition, we have analyzed the effects of shadowing on the rate selection problem along with Rayleigh fading. Our results indicate that shadowing can be supportive or destructive in terms of the expected throughput depending on the users' average SNRs.

These results are extended to cases where MUD capability is available at the receiver. In these scenarios, we model each collision as a MAC, and investigate the optimal rates and activity probabilities from an information theoretic perspective. The solutions for these cases are more complicated than those of the single user detection, hence we mostly resort to numerical optimization tools such as gradient descent and interior point methods. For throughput fairness, a four step method is introduced. We also discuss the convergence and global optimality of the provided solutions. In addition, we present detailed numerical examples illustrating our findings.

Our results reveal that the optimal rate selection for both MUD and no MUD cases offer better performance in terms of expected system throughput w.r.t. the same rate assumption among all the users (which is commonly used in the literature). Our method can be beneficial in practical scenarios for wireless sensor networking applications, machine to machine communications, etc. Our consideration of fairness in terms of throughput can also be beneficial in the applications where each user should have at least a minimum guaranteed throughput. In addition, the contribution on limiting the outage probabilities should be useful for delay constrained applications.

As further work, several directions can be followed. Firstly, one can investigate the optimal rate and activity probability selection for other wireless channel scenarios such as Rician fading and Nakagami fading. In addition, it can be also interesting to analyze the cases with frequency-selective fading and the scenarios where CSI is also available at transmitter side which may provide a significant increase in throughput.

One can also focus on more than 2-level MUD scenarios, and find the optimal rates as well. This could be an important approach to reveal the true potential of MUD. However, the receiver complexity would be an important challenge.

Another line of work can be on the delay analysis to evaluate the benefits of limiting individual outage probabilities in more detail. Moreover, an analysis on the total energy consumption can be performed. In addition, a system with energy harvesting users can also be considered, and optimal activity probabilities can be found depending on the each user's energy harvesting rate.

# Bibliography


[1] N. Abramson, "The ALOHA system: Another alternative for computer communications," in *Proc. Fall Joint Comput. Conf.*, (Houston, TX), pp. 281–285, Nov. 1970.

[2] L. G. Roberts, "ALOHA packet system with and without slots and capture," *SIGCOMM Comput. Commun. Rev.*, vol. 5, pp. 28–42, Apr. 1975.

[3] J. Metzner, "On improving utilization in ALOHA networks," *IEEE Trans. Commun.*, vol. 24, pp. 447–448, Apr. 1976.

[4] G. D. Nguyen, A. Ephremides, and J. E. Wieselthier, "On capture in random-access systems," in *IEEE Int. Symp. Inf. Theory*, (Seattle, WA), pp. 2072–2076, July 2006.

[5] Y. Li and L. Dai, "Effect of fading on maximum sum rate of ALOHA," in *Ann. Conf. Inf. Sci. Syst. (CISS)*, (Princeton, NJ), pp. 436–441, Mar. 2016.

[6] M. Mollanoori and M. Ghaderi, "On the performance of successive interference cancellation in random access networks," in *IEEE Sens., Mesh, Ad Hoc Commun. Networks Conf.*, (Seoul, Korea), pp. 461–469, June 2012.

[7] E. Casini, R. D. Gaudenzi, and O. D. R. Herrero, "Contention resolution diversity slotted ALOHA (CRDSA): An enhanced random access scheme for satellite access packet networks," *IEEE Trans. Wireless Commun.*, vol. 6, pp. 1408–1419, Apr. 2007.

[8] G. Liva, "Graph-based analysis and optimization of contention resolution diversity slotted ALOHA," *IEEE Trans. Commun.*, vol. 59, pp. 477–487, Feb. 2011.

[9] M. Medard, J. Huang, A. J. Goldsmith, S. P. Meyn, and T. P. Coleman, "Capacity of time-slotted ALOHA packetized multiple-access systems over the AWGN channel," *IEEE Trans. Wireless Commun.*, vol. 3, pp. 486–499, Mar. 2004.

[10] C. Wei, P. Fan, and K. B. Letaief, "On channel coding selection in time-slotted ALOHA packetized multiple-access systems over Rayleigh fading channels," *IEEE Trans. Wireless Commun.*, vol. 7, pp. 1699–1707, May 2008.

[11] T. Cui, T. Ho, and J. Kliewer, "Achievable rate and optimal physical layer rate allocation in interference-free wireless networks," in *IEEE Int. Symp. Inf. Theory*, (Seoul, Korea), pp. 2674–2678, June 2009.

[12] H. S. Dhillon, H. Huang, H. Viswanathan, and R. A. Valenzuela, "Fundamentals of throughput maximization with random arrivals for M2M communications," *IEEE Trans. Commun.*, vol. 62, pp. 4094–4109, Nov. 2014.

[13] P. Minero and M. Franceschetti, "Throughput of slotted ALOHA with encoding rate optimization and multipacket reception," in *Int. Conf. Comp. Commun.*, (Rio de Janeiro, Brazil), pp. 2971–2975, Apr. 2009.

[14] P. Minero, M. Franceschetti, and D. N. C. Tse, "Random access: An information-theoretic perspective," *IEEE Trans. Inf. Theory*, vol. 58, pp. 909–930, Feb 2012.

[15] C. Boyer and S. Dastangoo, "Random access with imperfect state information: An information theoretic approach," in *IEEE Int. Symp. Pers., Indoor, Mobile Radio Commun.*, (London, UK), pp. 1817–1822, Sept 2013.

[16] J. Yuan, T. Li, and M. Torlak, "Throughput optimization for cognitive radio under random access ALOHA networks," in *Texas Symp. Wireless Microwave Circ. Syst.*, (Waco, TX), pp. 1–5, Apr. 2015.

[17] G. Mergen and L. Tong, "Maximum asymptotic stable throughput of opportunistic slotted ALOHA and applications to CDMA networks," *IEEE Trans. Wireless Commun.*, vol. 6, pp. 1159–1163, Apr. 2007.

[18] G. Bartoli, N. C. Beaulieu, R. Fantacci, and D. Marabissi, "An effective multiuser detection scheme for mpr random access networks," *IEEE Trans. Commun.*, vol. 65, pp. 1119–1130, Mar. 2017.

[19] M. Koseoglu, E. Karasan, and L. Chen, "Cross-layer energy minimization for underwater aloha networks," *IEEE Syst. J.*, vol. 11, pp. 551–561, Jun. 2017.

[20] H. Yang and M. Alouini, "Throughput of slotted ALOHA systems in mixed Rician-Nakagami fading environments with a minimum signal power constraint," in *IEEE Int. Conf. Commun.*, vol. 6, (Helsinki, Finland), pp. 1723–1727, June 2001.

[21] I. Widipangestu, A. J. Jong, and R. Prasad, "Capture probability and throughput analysis of slotted ALOHA and unslotted np-ISMA in a Rician/Rayleigh environment," *IEEE Trans. Veh. Technol.*, vol. 43, pp. 457–465, Aug. 1994.

[22] S. A. Al-Semari and M. Guizani, "Channel throughput of slotted ALOHA in a Nakagami fading environment," in *IEEE Int. Conf. Commun.*, vol. 2, (Montreal, Canada), pp. 605–609 vol.2, Jun 1997.

[23] R. Prasad and J. C. Arnbak, "Effects of Rayleigh fading on packet radio channels with shadowing," in *IEEE Reg. 10 Int. Conf.*, (Bombay, India), pp. 546–548, Nov. 1989.

[24] T. T. Ha, "The effect of fading in mobile ALOHA radio communications," in *IEEE Vehicular Tech. Conf.*, (San Francisco, CA), pp. 19–21 vol.1, May 1989.

[25] R. Sámano-Robles, "Trade-off performance regions of random access protocols with multi-packet reception (MPR) via multi-objective optimization," in *Wireless Optical Commun. Conf. (WOCC)*, (Newark, NJ, USA), pp. 1–6, May 2014.

[26] H. Chang, V. Misra, and D. Rubenstein, "Fairness and physical layer capture in random access networks," in *IEEE Conf. Sensor, Mesh, Ad Hoc Commun. Networks*, (San Diego, CA), pp. 381–390, Jun. 2007.

[27] S. Sharifi, A. K. Tanc, and T. M. Duman, "LDPC code design for the two-user Gaussian multiple access channel," *IEEE Trans. Wireless Commun.*, vol. 15, pp. 2833–2844, Apr. 2016.

[28] L. Kleinrock and F. Tobagi, "Packet switching in radio channels: Part I - carrier sense multiple-access modes and their throughput-delay characteristics," *IEEE Trans. Commun.*, vol. 23, pp. 1400–1416, Dec. 1975.

[29] G. Choudhury and S. Rappaport, "Diversity ALOHA - a random access scheme for satellite communications," *IEEE Trans. Commun.*, vol. 31, pp. 450–457, Mar. 1983.

[30] Q. Peng, M. Zhang, and W. Wu, "Variant enhanced dynamic frame slotted ALOHA algorithm for fast object identification in RFID system," in *Int. Workshop Anti-Counterfeiting, Security, Identification*, (Xiamen, China), pp. 88–91, Apr. 2007.

[31] A. Goldsmith, *Wireless Communications*. New York, NY, USA: Cambridge University Press, 2005.

[32] D. Tse and P. Viswanath, *Fundamentals of Wireless Communication*. New York, NY, USA: Cambridge University Press, 2005.

[33] E. Biglieri, J. Proakis, and S. Shamai, "Fading channels: information-theoretic and communications aspects," *IEEE Trans. Inf. Theory*, vol. 44, pp. 2619–2692, Oct. 1998.

[34] T. M. Cover and J. A. Thomas, *Elements of Information Theory (Wiley Series in Telecommunications and Signal Processing)*. Wiley-Interscience, 2006.

[35] S. Verdu, *Multiuser Detection*. New York, NY, USA: Cambridge University Press, 1st ed., 1998.

[36] S. Boyd and L. Vandenberghe, *Convex Optimization.* New York, NY, USA: Cambridge University Press, 2004.